Relative Role of Uncertainty for Predictions of Southeastern U.S. Pine Carbon Cycling

Annika Lee Jersild

Thesis submitted to the faculty of the Virginia Polytechnic Institute and State University in partial fulfillment of the requirements for the degree of

Master of Science
In
Forestry

Robert Q. Thomas, Chair
Valerie A. Thomas
Thomas R. Fox

04/29/2016
Blacksburg, VA

Keywords: carbon sequestration, data assimilation (DA), Metropolis-Hastings Markov Chain Monte Carlo (MHMCMC), Bayesian Statistics, Loblolly Pine (*Pinus taeda*), pine plantation management, ecosystem modeling, identifying uncertainty, global climate models (GCMs)

Relative Role of Uncertainty for Predictions of Southeastern U.S. Pine Carbon Cycling

Annika Lee Jersild

ABSTRACT (academic)

Predictions of how forest productivity and carbon sequestration will respond to climate change are essential for making forest management decisions and adapting to future climate. However, current predictions can include considerable uncertainty that is not well quantified. To address the need for better quantification of uncertainty, we calculated and compared ecosystem model parameter, ecosystem model process, climate model, and climate scenario uncertainty for predictions of Southeastern U.S. pine forest productivity. We applied a data assimilation using Metropolis-Hastings Markov Chain Monte Carlo to fuse diverse datasets with the Physiological Principles Predicting Growth model. The spatially and temporally diverse data sets allowed for novel constraints on ecosystem model parameters and allowed for the quantification of uncertainty associated with parameterization and model structure (process). Overall, we found that the uncertainty is higher for parameter and process model uncertainty than the climate model uncertainty. We determined that climate change will result in a likely increase in terrestrial carbon storage and that higher emission scenarios increase the uncertainty in our predictions. In addition, we determined regional variations in biomass accumulation due to a response to the change in frost days, temperature, and vapor pressure deficit. Since the uncertainty associated with ecosystem model parameter and process uncertainty was larger than the uncertainty associated with climate predictions, our results indicate that better constraining parameters in ecosystem models and improving the mathematical structure of ecosystem models can improve future predictions of forest productivity and carbon sequestration.

Relative Role of Uncertainty for Predictions of Southeastern U.S. Pine Carbon Cycling

Annika Lee Jersild

ABSTRACT (General Audience)

Predictions of how forest productivity and carbon sequestration will respond to climate change are essential for making forest management decisions and adapting to future climate. However, current predictions can include considerable uncertainty that is not well quantified. To address the need for better quantification of uncertainty, we calculated and compared ecosystem model parameter, ecosystem model process, climate model, and climate scenario uncertainty for predictions of Southeastern U.S. pine forest productivity. We used mathematical techniques to improve model results and quantify uncertainty by incorporating observed data with ecosystem model results to quantify the uncertainty. Overall, we found that the uncertainty associated with the ecosystem model was higher than the uncertainty associated with the climate models. We determined that climate change will result in a likely increase in biomass accumulation in these loblolly pine forests. In addition, we determined regional variation due to the effects of changing frost days, temperature, and vapor pressure deficit. Since the uncertainty associated with ecosystem model parameter and process uncertainty was larger than what was associated with climate predictions, future research focused on and improving the mathematical structure of ecosystem models can improve future predictions of forest productivity.

ACKNOWLEDGEMENTS

This work was supported by Virginia Space Grant Consortium Graduate STEM Research Fellowship 2015-2016, USDA-NIFA Project #2015-67003-23485, and USDA National Institute of Food and Agriculture, Award #2011-68002-30185. I acknowledge Virginia Tech Advanced Research Computing, Forest Productivity Cooperative, and the Forest Modeling Research Cooperative. I thank members of the Thomas lab, Ben Ahlswede and Kevin Horn, and my family and friends for feedback and discussion. In addition I thank the following important contributors to my project: Evan Brooks, Robert Teskey, Randolph Wynne, David Sampson, Carlos Gonzalez, Luke Smallman, and especially my committee Thomas Fox, Valerie Thomas, and my advisor Quinn Thomas.

TABLE OF CONTENTS

List of figures

List of tables

Chapter 1: Introduction

Developing the capacity to accurately predict the impact of climate change on forest productivity and carbon sequestration is essential to understand the effects of climate change and the impact of future atmospheric carbon dioxide. Climate models and ecosystem models offer powerful tools in making predictions of both future climate and the impact of that climate on ecosystems. However, models used to predict forest carbon (C) uptake often are under-constrained by data and do not include comprehensive estimates of uncertainty. To forecast the influence of climate change and rising atmospheric carbon dioxide (CO_2) on forest productivity and to quantify the associated uncertainty, we applied data assimilation (DA) techniques to integrate diverse data sources into an ecosystem model. We then used the uncertainty estimates from the DA to quantify four different sources of uncertainty in the forecast: ecosystem model parameter, ecosystem model process, climate model, and climate scenario.

Many ecosystem studies have quantified uncertainty in predictions, but few have integrated their findings across multiple types of uncertainty. Many studies focus on the sensitivity of a single uncertainty source, or identify how the uncertainty in the output can be attributed to specific sources of uncertainty in the inputs. Previous research efforts have analyzed parameter sensitivity (Gardner et al. 1981, Esprey et al. 2004, Gao et al. 2011, Weng and Luo 2011), process model sensitivity (Cramer et al. 2001, Morales et al. 2005, van Oijen and Thomson 2010), and climate model sensitivity (Murphy et al. 2004, Olesen et al. 2007), but none of this literature analyzes which of these uncertainty sources has the greatest impact within a single forecast. Focusing only on uncertainty in model parameters, Gao et al (Gao et al. 2011) analyzed the effect of incorporating a DA method to improve forecasts of forest carbon dynamics. Their results, showing an improvement in parameterization using more data sources and a data assimilation method, emphasized the ability of the DA method to improve forest carbon dynamics predictions, constrain parameters, and evaluate uncertainty. Van Oijen et al (van Oijen et al. 2005) also used a DA and a Bayesian statistical method in order to quantify uncertainty and more accurately calibrate process-based forest models. Their research highlights how increasing the variety of data and employing Bayesian calibration methods can reduce parameter and output uncertainty in forest models. Studies to date that focus on the need for

quantifying uncertainty (van Oijen et al. 2005, Ascough et al. 2008, Luo et al. 2009) demonstrate the need for and importance of research that compares how the different components (i.e. model inputs, parameters, and model structure) contribute to prediction uncertainty.

Predicting the change in biomass accumulation over time and quantifying the uncertainty in those predictions for these forest ecosystems is particularly important for the Southeast United States. Forest ecosystems will be slow to respond to climate change because of the size and life span of trees, and multi-decade forest plantations cannot be shifted geographically as quickly as crops (Loehle and LeBlanc 1996). Making predictions of how climate change will affect forests is essential to maintain the industry and the economy of forested regions. Pine plantation ecosystems in the Southeastern U.S. are of particular interest because they are among the most intensively managed and fastest growing ecosystems in the world (Fox et al. 2007) and have been extensively studied using region-wide observational and manipulative studies. The combination of region-wide observations that cover a range of climates and experimental manipulations of nutrition and CO_2 are ideal for developing model parameterization through DA that can be used to predict ecosystem response to climate and atmospheric CO_2 change. Furthermore, the pine plantations commonly are mono-specific (loblolly pine; *Pinus taeda L.*) allowing for increased confidence in region-wide parameterization from data assimilation. Finally, southern pine ecosystems absorb a large fraction of the U.S. carbon uptake (Turner et al. 1995), highlighting the need to forecast how carbon uptake in the systems will change in the future. Making predictions for the change in biomass over time in loblolly pine plantations in the southeast U.S. with the changing climate and identifying which sources of uncertainty have the greatest influence on this prediction will allow for more robust forecasts of future loblolly pine plantation growth. In addition, it will allow for future research to better identify areas where reducing uncertainty and improving methods could exert considerable influence in creating more accurate forecasts.

Chapter 2: Background Information

2.1 Forest Carbon Storage & Influence on Climate

Forest ecosystems play a critical role in the global climate by absorbing carbon dioxide from the atmosphere. Understanding the forest carbon (C) sink and being able to make accurate forest carbon storage predictions for the future are important for efficient and environmentally

beneficial planning of forest ecosystems. Forests cover ~4.1 billion hectares of the Earth's land surface globally, and about 42% of the global forest C stock is contained in live forest biomass (Pan et al. 2011). As forests grow, they store C by absorbing atmospheric carbon dioxide (CO_2) through photosynthesis and converting it to cellulose, sugars, and carbohydrates used for growth. This uptake of CO_2 reduces the atmospheric concentrations of CO_2, and influences both the speed and the magnitude of human-induced climate change. Globally, forest net growth (biomass accumulation in forests) absorbs about 30% of all CO_2 emissions from fossil fuel burning and net deforestation (Canadell et al. 2007). This terrestrial carbon sink is in the range of 2.0 to 3.4 PG C/year worldwide (Bonan 2008, Pan et al. 2011). However, this sink varies regionally with areas of carbon sources and areas of carbon sinks (Canadell et al. 2007). Understanding the carbon storage trends regionally will prove important to understanding and predicting global patterns and future climate impacts. Any future changes in the storage of C by forests can have an indirect influence on climate and understanding these changes could prove essential to effective climate change mitigation efforts.

2.2 Uncertainty in Predictions

Uncertainty is defined as something that is unknown or unsure (Merriam-Webster); uncertainty in models is attributable to sources of error, variability, or the inherent uncertainty associated with mathematical representations of the future. Essentially, quantifying uncertainty allows for model predictions to be more useful by providing a measure of the certainty associated with the prediction. Uncertainty is a term that can be attributed to a wide variety of sources, and there is no scientific consensus on exactly which forms of uncertainty must be incorporated into a prediction (Ascough et al. 2008). However, it is recognized that improving quantification of uncertainty improves predictions and the ability to use predictions for future decision making processes (Ascough et al. 2008, Dietze et al. 2013). Although there are many forms of uncertainty that have an effect on carbon storage predictions over the next 100 years, four major types of uncertainty to consider are climate scenario, climate model, ecosystem model parameter uncertainty, and ecosystem model process uncertainty.

2.2.1 Climate Scenario Uncertainty

The magnitude of climate change and the potential effect on forest carbon cycling strongly depends on the magnitude of human emissions over the 21st century. The

Intergovernmental Panel on Climate Change (IPCC, an international body for assessing the science related to climate change) uses Representative Concentration Pathways (RCPs) to represent plausible trajectories of emissions (Nakicenovic et al. 2000). RCP 8.5 is the scenario with the highest emissions where emissions continue to increase throughout the 21st century to reach a CO_2 concentration in the atmosphere of approximately 900 ppm by the end of the century. RCP 6.0, RCP 4.5, and RCP 2.6 represent scenarios where emissions peak between 2025 and 2030. RCP 4.5 is commonly used in ecosystem modeling as a contrast to RCP 8.5 because it represents a lower-emission scenario that assumes collective climate mitigation and a peak emission level by 2040. This peak is followed by a decrease in emissions following 2040. RCP 4.5 estimates atmospheric CO_2 concentration to be closer to 540 ppm by the end of the century. Current atmospheric CO_2 concentration levels are around 400 ppm, so there would need to be significant mitigation efforts to achieve the levels set in RCP 4.5. In order to incorporate this variability of climate results from human actions it is necessary to analyze both the high and the low emission scenarios.

2.2.2 Climate Model Uncertainty

Predictions of future forest dynamics depend on model simulations of future climate using global climate models (GCMs). Comprehensive GCMs are one of the few tools that can be used to determine future climate change at both global and regional levels. GCMs simulate key physical processes to represent the complex, nonlinear interactions that effect climate change at a regional level (Murphy et al. 2004). These models vary widely, predicting a range of values and incorporating various levels of atmospheric, earth system, ocean, carbon cycle, and biogeochemical interactions (Randall and Wood 2007). For example, RCP 4.5 predicts a change of 2-3°C by 2100, and RCP 8.5 predicts a global temperature change of 4-6°C by 2100, depending on the model used to make the prediction (Intergovernmental Panel on Climate Change 2014). These differences in climate model structure can result in prediction uncertainty as the models can have a range of predictions despite equivalent model input. In some cases, the uncertainties between models result in disagreement on the sign of the changes that could result in a particular region.

2.2.3 Ecosystem Model Parameter Uncertainty

Ecosystem models are one of the primary tools used to quantify the regional predictions of future forest carbon dynamics, but they often lack estimates of uncertainty. Ecosystem models

have become increasingly complex, attempting to mathematically represent as much of the natural world interactions as possible (Clark and Gelfand 2006). This complexity can result in an increased number of parameters required to run the model. However, an important critique of process-based ecosystem models has been that they require too many poorly known parameters in order to make reliable predictions, and as such they have too much uncertainty (Mohren and Burkhart 1991). This lack of known parameters can lead to the model being too subjective, or not adequately quantifying real-world dynamics or estimates of uncertainty (Luo et al. 2011). In order to capture this error, we quantified the uncertainty associated with ecosystem model parameters by estimating distribution of values for each parameter that are consistent with observations. We then made predictions using a range of possible parameter values and their likelihoods instead of using a single value to represent that parameter.

2.2.4 Ecosystem Model Process Uncertainty

In addition to the ecosystem parameter uncertainty, the structure of the model (i.e. which equations are used) inherently has error so that no set of parameters can perfectly explain observations. This inherent uncertainty stems from simplifying biological and physical processes with a mathematical equation, defined as process uncertainty. Process-based ecosystem models are beneficial because they represent a simulated ecological system and allow predictions into the future; however, the disadvantage to building this representative model is the intrinsic subjectivity incorporated through the process of building the model (Williams et al. 2005). Models built too simply do not accurately represent a system; models built too complex leave room for increased error and parameterization complications (Ascough et al. 2008). Ecosystem model uncertainty can be estimated by two approaches. First, predictions from an individual ecosystem model can be compared to observations to estimate standard deviation of the model fit. Second, multiple independent ecosystem models run with the same climate input data can be used to compare the spread of model predictions as an estimate of uncertainty. Here we focused on the former approach for quantifying model process uncertainty using a single ecosystem model, the Physiological Principles Predicting Growth (3-PG) model.

2.3 Method of Quantifying Uncertainty

Uncertainty is found in all models and predictions, and is usually quantified using statistical methods. The two main forms of statistical analysis are frequentist and Bayesian statistical approaches. The key difference between frequentist and Bayesian statistics lies in their

approach to calculating a probability. Frequentists calculate data based on repeated, random measurements, so the probability is tied to the frequency of the event. Essentially, probability is evaluated as the relative frequency with which an event occurs given repeated trials. The parameters are fixed, and they use confidence intervals (a 95% confidence interval means that out of 100 samples, 95 of them will be within that sample). For Bayesians, in contrast, probability is related to knowledge about an event, and the data is observed from samples and is fixed while the parameters are unknown and probabilistically calculated. The Bayesian concept of probability focuses more on the degree of certainty about a statement, and they use credible intervals instead of confidence intervals (a 95% credible interval means that there is a 95% probability that your value is within that credible interval range). This difference in philosophy leads to dramatically different statistical techniques, with Bayesian techniques based on Bayes theorem. According to Bayes theorem, the unknown probability of a parameter value is proportional to the prior probability of the parameter times the probability of the collective data given that parameter value (Ogle and Barber 2008). Bayesian statistics focuses on outputting the estimation of unknown parameters (in the form of a distribution), using these prior beliefs expressed as probability density functions (Qian et al. 2003). The Bayesian method is increasing in popularity among the sciences due to the way it incorporates prior information, explicitly handles uncertainty, and has the ability to assimilate new information useful for concepts such as adaptive management (Qian et al. 2003).

Data assimilation (DA) is the general term for statistical methods that optimize the combination of models, prior knowledge, and measurements to provide a better estimate of system dynamics than either one could supply on its own (Williams et al. 2005). Data assimilation techniques are often Bayesian in nature as they are focused on estimating the posterior distribution of model parameters. These posterior distributions are used to develop probabilistic predictions (i.e., ecological forecasting) that include estimates of uncertainty. DA improves these ecological forecasts and uncertainty estimates by combining models of ecological processes with data and observations in order to improve ecological predictions, identify sources of error, and more rigorously constrain model parameters (Hobbs and Ogle 2011, Luo et al. 2011, Niu et al. 2014).

A key challenge for DA and Bayesian statistics in general is the numerical approzimation of an unknown posterior distribution. The Metropolis-Hastings Markov Chain Monte Carlo

(MHMCMC) is a common used computer algorithm to approximate the posterior distribution of parameters from known prior distributions and a known likelihood of the data given the parameters (Xu et al. 2006, Hill et al. 2011, Bloom and Williams 2015). The Markov Chain Monte Carlo algorithm is the general method that samples from prior distributions with multiple iterations to output the parameter probability distributions. The MHMCMC algorithm uses MCMC sampling process but accepts or rejects certain steps based on likelihood values, generating posterior distributions of the target variables that can be used to determine mean values, credible intervals, and summaries of uncertainty (Luo et al. 2011).

2.4 The Physiological Principles Predicting Growth Model

In order to make the ecosystem predictions and incorporate data assimilation to improve predictions, process-based ecosystem models with relatively few parameters are ideal. Here, we used the Physiological Principles Predicting Growth (3-PG) model. The 3-PG model is a stand growth model that calculates total carbon fixed based on physiological processes (Landsberg and Waring 1997). 3-PG is a simplified, process-based growth model, which means it is based on mechanisms that underlie growth, and it is responsive to environmental or site condition changes (Pinjuv et al. 2006).It is used worldwide for projections of regional productivity and plantation management decisions (Mäkelä et al. 2000, Coops and Waring 2001, Landsberg et al. 2003, Bryars et al. 2013). The model uses a number of relationships derived from field research, combining process-based calculations with allometric and empirical relationships to ultimately produce variables of forest growth estimates such as leaf area index (LAI) or basal area (BA) (Coops 1999).

The key aspects of the 3-PG model that relate to predictions of forest dynamics under future climate and CO_2 are the temperature response function (fT), the vapor pressure deficit modifier (fVPD), the soil model water modifier (fSW), the frost modifier (fFrost), and the atmospheric CO_2 modifier (fCalpha). These environmental modifiers use parameters in an equation with environmental variables (from the climate predictions, site location, and atmospheric CO_2 levels) to adjust use efficiency and biomass accumulation at that site. The temperature response function is a hump-shaped function with an optimum (Topt), a minimum (Tmin), and a maximum (Tmax) temperature of photosynthesis (Figure 3a). The VPD modifier is an exponential function where the LUE decreases with an increasing VPD based on the CoeffCond parameter (Figure 3b). The soil water modifier is a logistic function of the ratio of

ASW to MaxASW, using the SWconst and SWpower parameters (Figure 3c). The frost modifier is linear and is proportional (based on kF) to the fraction of frost days that month—an increased amount of frost days means a lower value for the frost modifier (Figure 3d). Finally, the atmospheric CO_2 modifier is a saturating function of atmospheric CO2 using a parameter that represents the increase in light use efficiency associated with the increase in CO2 from 350 to 700 ppm (Figure 3e).

2.5 Objectives

The objective of this research was to improve quantification of uncertainty in predictions of carbon storage for loblolly pine plantations in the southeast U.S. This study quantified the sources of uncertainty using a data assimilation process in order to answer the following questions. 1) What is the predicted change in biomass over time at loblolly pine plantations with the effects of changing climate? 2) Which source of uncertainty out of ecosystem model parameter uncertainty, ecosystem model process uncertainty, climate model uncertainty, and climate scenario uncertainty has the greatest influence on this prediction? Answering these questions while employing the data assimilation and a Bayesian statistical technique allowed for more robust forecasts of future loblolly pine plantation growth. In addition, the results can be applied for future research to better identify areas where reducing uncertainty and improving methods could make the greatest influence on forecasting.

Chapter 3: Materials & Methods

3.1 Data Assimilation: DAPPER, MHMCMC, & 3-PG

We used the Data Assimilation for Pine Planation Ecosystem Research (DAPPER) to handle the diverse data sources, calibrate the 3-PG model, and calculate prediction uncertainty (Thomas, Jersild et al, in prep). DAPPER uses data assimilation and the Bayesian statistical method Metropolis-Hastings Markov Chain Monte Carlo (MHMCMC) to use diverse data sources to calibrate the 3-PG ecosystem model and estimate posterior distributions for the model parameters. These posterior distributions, including distributions on the standard deviation of the model fit, were used to estimate uncertainty in biomass predictions due to parameterization and due to model fit (i.e. standard deviation of model fit). These distributions were then used with the 3-PG model and future climate data projections in order to make forecasts of future ecosystem

growth and carbon storage at a selected site of interest. The distributions gave us more accurate estimates of parameter values as well as the uncertainty surrounding those values, allowing for more accurate and robust predictions of future biomass.

In order to use Bayes Theorem to estimate the posterior distribution of model parameter, the prior distributions for the parameters had to be specific and the likelihood of the observations given the parameters needed to be calculated. The prior distributions for the model parameters are listed in Table 1 and were derived from previous parameterizations of the 3-PG model, from the literature, or are intentionally set to be vague. We set priors on the parameters to be uniform with ranges based on either literature values or set to be a large range to be vague (Figure 2a). In a few cases, we used normal prior distributions when supported by the literature. The likelihood (i.e., the cost function) was normally distributed with a standard deviation parameter associated with each data source described below.

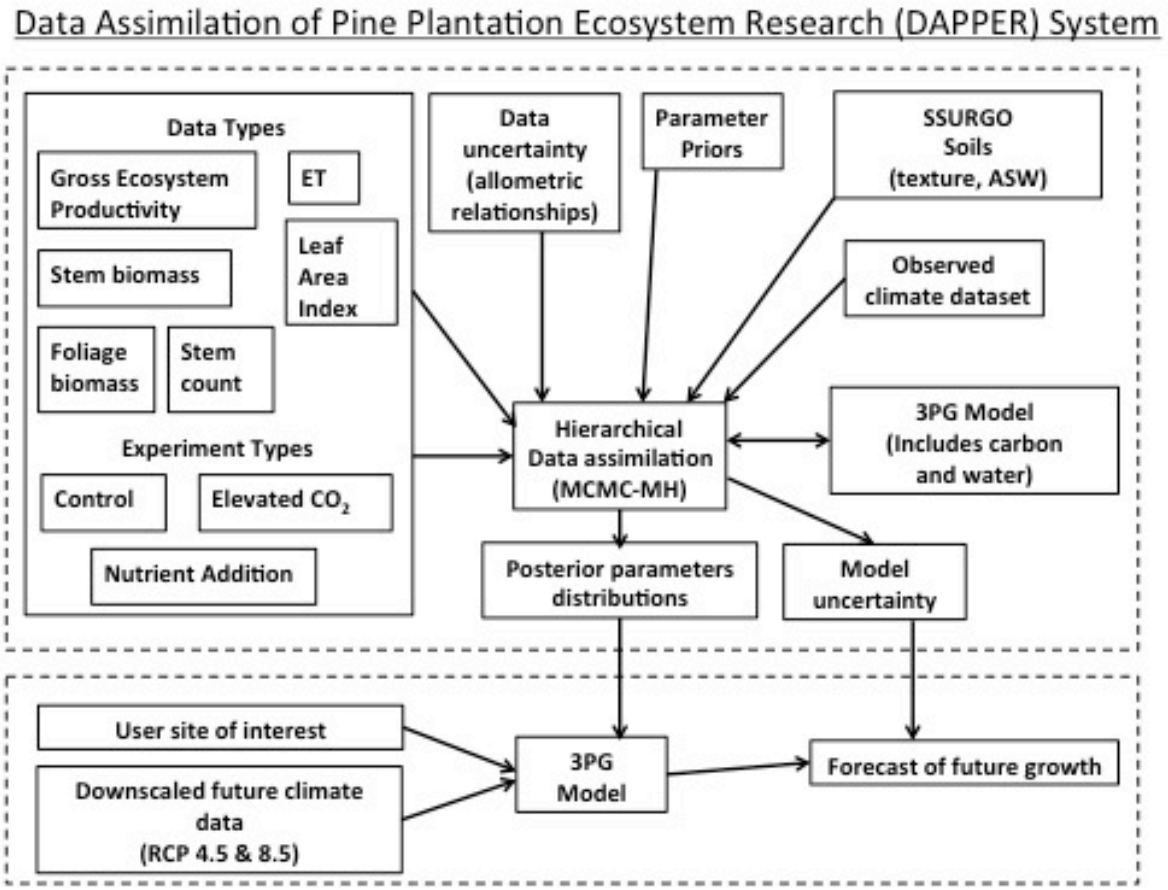

Figure 1*: Inputs and Outputs of the DAPPER system, developed by Thomas and Jersild et al. Shows incorporation of data types, parameter priors, data uncertainty, and climate & site data into the hierarchical data assimilation, which outputs the parameter posterior distributions and the model uncertainty incorporated to analyze uncertainty in forecasts of future growth.*

Table 1: Prior distributions set based on expert opinion and accepted values. The Uniform distributions have a minimum and maximum, with an equal probability placed on all values within that range. The normal distributions instead have a mean and a standard deviation around that mean, representing values closer to the mean having a higher likelihood than those at the edge of the standard deviation. Each prior has an initial value, and if fixed does not use the MHMCMC chain and instead stays at that initial value.

Prior	Minimum	Maximum	Initial Value	Distribution	Fixed or Not Fixed
pFS2	0.08	1.5	0.55	Uniform	Not Fixed
pFS20	0.1	1.5	0.40	Uniform	Not Fixed
StemConst	0.022 (mean)	0.05 (SD)	0.022	Normal	Not Fixed
StemPower	2.77 (mean)	0.2 (SD)	2.77	Normal	Not Fixed
pRx	0.2	0.72	.65	Uniform	Not Fixed
pRN	0.04	0.5	0.36	Uniform	Not Fixed
SLA0	5.43 (mean)	0.44 (SD)	5.43	Normal	Not Fixed
SLA1	3.58 (mean)	0.11 (SD)	3.58	Normal	Not Fixed
tSLA	5.97 (mean)	2.15 (SD)	5.97	Normal	Not Fixed
k	0.55	0.60	0.56	Uniform	Not Fixed
fullCanAge	2	8	3	Normal	Fixed
MaxIntcptn	0.14	0.22	0.2	Normal	Fixed
LAImaxIntcptn	2	6	5	Normal	Fixed
alpha	0.2	0.6	0.041	Normal	Not Fixed
MaxCond	0.001	0.011	0.006	Normal	Not Fixed
LAIgcx	2.5	4.0	3.2	Normal	Not Fixed
CoeffCond	0.013	0.038	0.036	Normal	Not Fixed
BLcond	0.02	0.18	0.1	Normal	Fixed
wSx1000	235 (mean)	25 (SD)	235	Uniform	Not Fixed
thinPower	1	2.5	1.75	Uniform	Fixed
mF	0.4	1	0.70	Uniform	Not Fixed
mR	0.001	0.5	0.3	Uniform	Fixed
mS	0.4	1	0.75	Uniform	Not Fixed
fracBB0	0.1	0.6	0.35	Uniform	Fixed
fracBB1	0.02	0.18	0.12	Uniform	Fixed
tBB	3	27	12	Uniform	Fixed
gammaFx	0.036	0.08	0.042	Uniform	Fixed
gammaF0	0.036	0.08	0.041	Uniform	Fixed
tgammaF	3.6	32.4	18	Uniform	Fixed
Rttover	0.005	0.08	0.025	Uniform	Not Fixed
m0	0.02	0.18	0.1	Uniform	Not Fixed
fN0	0.1	0.9	0.5	Uniform	Not Fixed
Tmin	4 (mean)	2 (SD)	4	Normal	Not Fixed
Topt	25 (mean)	2 (SD)	25	Normal	Not Fixed
Tmax	38 (mean)	2 (SD)	28	Normal	Not Fixed
kF	0.85	1	0.86	Uniform	Not Fixed
MaxAge	16	501	500	Uniform	Not Fixed

nAge	0.6	5.4	1.5	Uniform	Not Fixed
rAge	0.06	100	50	Uniform	Not Fixed
y	0.44 (mean)	0.015 (SD)	0.45	Normal	Not Fixed
Density	0.1	0.9	0.42	Uniform	Fixed
formFactor	0.09	0.81	0.45	Uniform	Fixed
volRatio	1.0	2.25	1.25	Uniform	Fixed
Qa	-162	-18	-90	Uniform	Fixed
Qb	0.16	1.44	0.8	Uniform	Fixed
gDM_mol	20	30	24	Uniform	Fixed
molPar_MJ	2	2.5	2.3	Uniform	Fixed
fCalpha700	1	2	1.25	Uniform	Not Fixed
fCg700	0.2	1.8	1	Uniform	Fixed
SWconst1	0.7	0.9	0.8	Uniform	Fixed
SWconst2	0.05	0.25	0.1	Uniform	Not Fixed
SWpower1	10	12	11	Uniform	Fixed
SWpower2	0.04	2.5	2.0	Uniform	Not Fixed
mort_rate	8.3e-6	8.3e-6	9.0e-4	Uniform	Not Fixed
alpha_h	0.01	0.06	0.05	Uniform	Not Fixed
pFS_h	0.2	2.0	0.4	Uniform	Not Fixed
pR_h	0.2	0.72	0.4	Uniform	Not Fixed
mort_rate_h	0.00001	0.002	0.001	Uniform	Not Fixed
SLA0	16 (mean)	3.8 (SD)	16	Normal	Fixed

To calculate the posterior distribution of model parameters from the priors and likelihood, we used the MHMCMC numerical method that commonly is applied in statistical research (Fox et al. 2009, Zobitz et al. 2011, Santaren et al. 2014). The MHMCMC is an iterative technique that 1) randomly selects a new parameter value (or set of parameter values) based on the current (or initial) parameter values, 2) calculates the product of the likelihood of the observations given the new parameters and probability of the new parameters given the prior distribution, and 3) compares the product of the likelihood and prior to the product from the previous parameter set. If the product had a higher probability than the previous parameter set, the new parameter set was accepted. If the product had a lower probability than the previous parameter set, the new parameter was accepted in proportion to the ratio of the new parameter probability to the previous probability (i.e. a 10% worse parameter set will be accepted 90% of the iterations). This allowed for slightly worse parameter sets to be accepted but substantially worse sets to be rejected. The iterative process exploring parameter space through accepting and rejecting parameter sets converges a sequence of values that represents random draws from the

posterior distribution (Figure 2c) (Hobbs et al. 2015). This chain formed the posterior distribution, which we used for future predictions to incorporate an accurate distribution of the most likely values of each parameter (Figure 2d). In our case, the chain was run for 30 million iterations to reach convergence. Examples of posterior distributions for key parameters that govern the environmental functions in 3-PG (see Introduction) can be found in Figure 3.

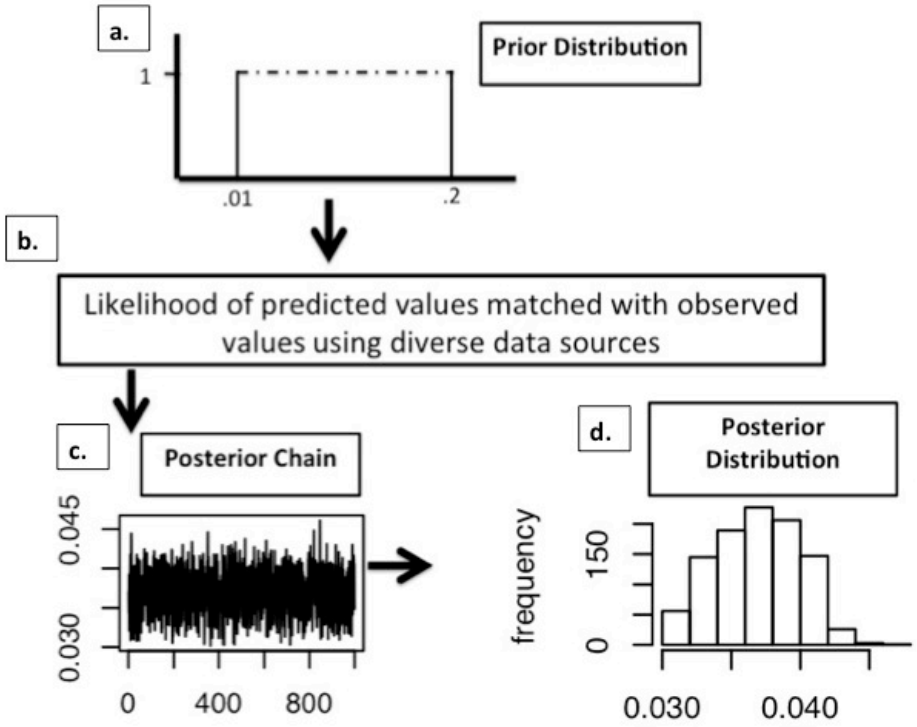

Figure 2*: Sample of a single iteration of the Metropolis-Hastings Markov Chain Monte Carlo Data Assimilation. This sample demonstrates the steps taken each iteration of our MHMCMC code built for the DAPPER system. (a) sample from the prior distribution for a specific parameter based on research and expert opinion, (b) calculate the likelihood of the value, (c) generate a posterior chain but continuing to iterate through and sample from the prior distribution, generating more values with higher likelihoods, (d) use that chain to form the posterior distribution. This is iterated multiple times for each parameter to generate a posterior distribution for each parameter in the model.*

We used the DAPPER system to develop posterior parameter distributions for the 3-PG Model (see Chapter 1 for a description). We fit 36 of the 59 parameters required by 3-PG, focusing the parameters that are associated with the growth response to climate change and

atmospheric CO_2. We also estimated posterior distributions for the site fertility (FR) at each plot in the observed data by fitting a specific FR parameter. This increased the total number of parameters by the number of field plots used in the DA. When fitting FR we required the FR of fertilized plots to be equal to or greater than the FR of corresponding control plots. We initialized the model simulation of each field plot at the age of first observation and used the first observation as initial conditions. A more complete description of the 3-PG model used in DAPPER can be found in Bryars et al. 2013 (Bryars et al. 2013).

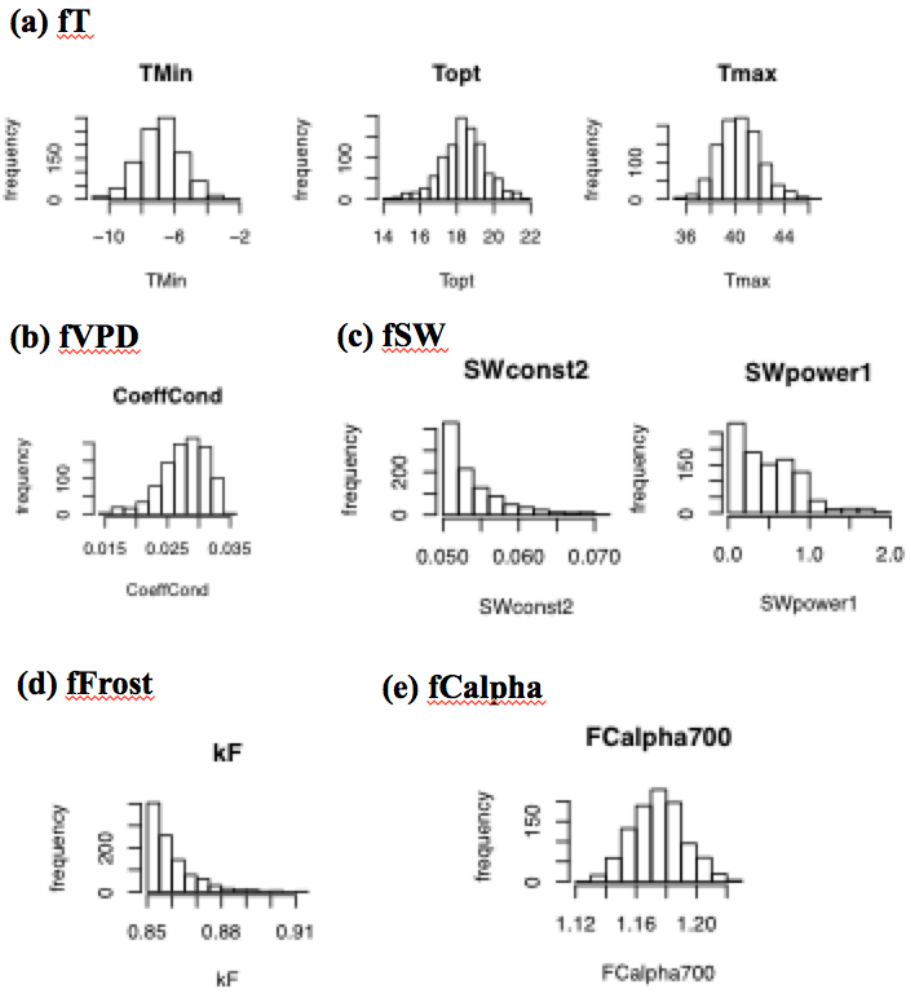

***Figure 3**: The parameter probability distribution output from the data assimilation for each parameter that has a large impact on the environmental modifiers in the 3-PG model. These parameters have an impact on the regional variability in biomass predictions. (a) temperature response modifier fT, (b) vapor pressure deficit modifier fVPD, (c) soil moisture water modifier fSW, (d) frost days modifier fFrost, (e) atmospheric CO_2 modifier fCalpha.*

3.2 Data Sources

The DAPPER system can include multiple streams of observations data to calculate the likelihood of the observations given parameters and to estimate the posterior distribution of the parameter. By including data that varies spatially by spanning the Southeastern U.S. and temporally by including observations from 1978 to 2015, the model parameters posteriors reflect diverse conditions where loblolly pine plantations occur. Furthermore, by including plots that received experimental manipulation of atmospheric CO_2 and nutrients, we were able to isolate key parameters in the 3-PG model associated with changing climate and atmospheric CO_2. Specifically, we used annual (or periodic) stem biomass, annual (or periodic) stem count, stand age, and leaf area index observations from 256 forest stands across the region. All sites included the stem biomass, stem count, and stand age observations with only a subset of sites reporting leaf area index. Thirty-five of the stands included a paired nutrient addition experiment that allowed for the site fertility parameter (FR) to be set to one (Forest Productivity Cooperative Region-wide 18 study; Fertilization study at Duke FACE; Fertilization treatments in the PINEMAP Tier 3 studies). Five of the stands included CO_2 that was experimentally elevated to 560 ppm (one of the CO_2 stands also included nutrient addition (Schlesinger et al. 2006). Two sites included monthly gross ecosystem productivity (i.e. gross primary productivity estimated from a flux tower) and monthly evapotranspiration (Duke Flux tower and NC2 flux tower). Data were collected by the Forest Productivity Research Cooperative, Forest Modeling Research Cooperative, Pine Integrated Network: Education, Mitigation, and Adaption project (PINEMAP), Duke CO_2 FACE project, and Ameriflux site researchers.

For each site we used soil texture and available soil water in the top 1.5 m from the Soil Survey Geographic (SSURGO) database (http://websoilsurvey.ncrs.usda.gov/). As climate inputs, we used the 4-km climate data from the METDATA gridded surface metrological dataset (Abatzoglou 2013) to determine the monthly values for minimum daily temperature, maximum daily temperature, number of frost days per month, monthly precipitation, and monthly mean daily solar isolation for each plot.

For future climate data, we used downscaled model output from twenty climate models that contributed to the CMIP5 project. The University of Idaho downscaled the data using the Multivariate Adaptive Constructed Analogs (MACA) statistical downscaling method

(http://maca.northwestknowledge.net/). We used the 4-km gridded downscaled climate predictions (2006-2100) for both RCP 4.5 and 8.5.

3.3 Calculations of Prediction Uncertainty

We partitioned uncertainty into parameter uncertainty, process model uncertainty, climate model uncertainty, and climate scenario uncertainty. Parameter uncertainty corresponds to the posterior distribution of the model parameters. We estimated the uncertainty in model predictions of total biomass in trees using bootstrapping. Specifically, we randomly selected a set of parameters from the parameter chain produced by the data assimilation methods described above and using 3-PG to predict the total biomass for that parameter set. By repeating the random selection for 1000 iterations, we approximated the probability distribution of total carbon at each stand age for a particular site that is attributable to uncertainty in the model parameters. We focused on the median value, the standard deviation of the distribution, and the 95% credible interval from the distribution (Code in Appendix A).

We quantified the ecosystem model process uncertainty by adding the normally distributed process error, represented as the estimated standard deviation on the likelihood calculation for a particular data type, to the total biomass estimates from the parameter uncertainty calculation. The model process uncertainty was also calculated using the median parameter distribution values to isolate the model process uncertainty alone. This uncertainty was incorporated into the results to calculate the median, standard deviation, and the 95% credible interval.

In addition to the uncertainty involved with the ecosystem model parameters and process, we estimated the uncertainty in total biomass predictions that is associated with uncertainty in predictions of future climate. We quantified the uncertainty in climate model predictions for a given scenario (climate model uncertainty) by using the MACA model output from 20 different climate models. To isolate climate model uncertainty, the ecosystem parameters were held at the median values of the probability parameter distributions and the ecosystem model process uncertainty was not incorporated. The distribution of results from the 20 different climate models were used to calculate the median, standard deviation, and the 95% credible interval associated with climate model uncertainty.

We quantified climate scenario uncertainty by including two potential representative concentration pathways (RCPs) identified by the IPCC: RCP 4.5 and RCP 8.5. RCP 4.5 represents a low-emission scenario with humans beginning climate change mitigation immediately, and RCP 8.5 represents a high-emission, business-as-usual scenario. We did not calculate a probability distribution, standard deviation, or 95% credible interval for climate scenario uncertainty because the scenarios are random samples from a distribution of potential scenarios.

Table 2: Global Climate Model Details. Lists each model incorporated as well as specific model details. ESM means it is an Earth System Model, with the capability to represent biogeochemical processes that interact with physical.

Model Name	Model Details	Citation
bcc-csm1-1	Beijing Climate Center Climate System Model, coupled climate-carbon model including vegetation and global C cycle. Low atmospheric resolution, 2.8° x 2.8°	(Feng et al. 2012)
bcc-csm1-1-m	Beijing Climate Center Climate System Model, with a moderate atmospheric resolution, 1.12° x 1.12°	(http://forecast.bcccsm.ncc-cma.net/web/channel-63.htm)
BNU-ESM	Beijing Normal University – fully coupled ESM	(Ji et al. 2014)
CanESM2	Canadian ESM – couples atmosphere-ocean, land-vegetation, terrestrial and oceanic interactive carbon cycle	(Chylek et al. 2011)
CCSM4	Community Climate System Model (USA) – general circulation climate model with atmosphere, land, ocean, and sea ice components	(Gent et al. 2011)
CNRM-CM5	National Centre of Meteorological Research, France - ESM consisting of several existing models coupled through OASIS software	(Mélia 2002)
CSIRO-Mk3-6-0	Australia - coupled atmosphere-ocean GCM	(Rotstayn et al. 2012)
GFDL-ESM2M	NOAA, USA - ESM, physical ocean component version 1	(Dunne et al. 2012)
GFDL-ESM2G	NOAA, USA - ESM, physical ocean component version 2	(Dunne et al. 2012)
HadGEM2-ES	Hadley Global Environmental Model - Earth System components	(Bellouin et al. 2007)
HadGEM2-CC	Hadley Global Environmental Model - Carbon Cycle components	(Bellouin et al. 2007)
inmcm4	Russia – coupled model of atmospheric and oceanic general circulations	(Volodin et al. 2010)

IPSL-CM5A-LR	Institute Pierre Simon Laplace, France – ESM, low atmospheric resolution, 3.75° x 1.9°	(Dufresne et al. 2013)
IPSL-CM5A-MR	Institute Pierre Simon Laplace, France – ESM, medium atmospheric resolution, 2.5° x 1.25°	(Dufresne et al. 2013)
IPSL-CM5B-LR	Institute Pierre Simon Laplace, France – ESM, atmospheric model with different parameterizations, low resolution	(Dufresne et al. 2013)
MIROC5	Model for Interdisciplinary Research on Climate, Japan – atmosphere-ocean GCM	(Watanabe et al. 2010)
MIROC-ESM	Model for Interdisciplinary Research on Climate, Japan – MIROC5 with ESM	(Watanabe et al. 2011)
MIROC-ESM-CHEM	Model for Interdisciplinary Research on Climate, Japan - ESM, includes coupled atmospheric chemistry component	(Watanabe et al. 2011)
MRI-CGCM3	Meteorological Research Institute, Japan – atmosphere-land, aerosol, and ocean ice models with subset of MRI's ESM	(Yukimoto et al. 2012)
NorESM1-M	Norwegian ESM – global, coupled model system with unique code for chemistry-aerosol-cloud radiation interactions	(Bentsen et al. 2013)

3.4 Model Simulations & Analysis

3.4.1 Site Selection

We focused our analysis on identifying and quantifying each type of uncertainty affecting a forecast at four sites across the Southeastern U.S. We selected four Tier III PINEMAP plots, located in Florida (30.206 N, -83.868 W), Oklahoma (34.031 N, -94.822 W), Georgia (33.626 N, -82.8 W), and Virginia (37.444 N, -78.664 W) (Figure 4). These sites were selected for their proximity to each of the edges of the native range of loblolly pines and their range across the native range of loblolly pines. The Florida plot, planted in 2004, had a mean minimum surface temperature of 14°C and a mean maximum temperature of 27°C, with a daily average precipitation of 105. The Oklahoma plot was planted in 2008 had a mean minimum surface temperature of 10.7°C, a maximum of 24.5°C, and a daily mean precipitation of 110.8. The Virginia plot was planted in 2003, and had a maximum mean surface temp of 20.4°C and a minimum of 6.5°C, and an average precipitation of 88.3. The Georgia plot was planted in 2006, and had a maximum temperature mean of 24.1°C, a minimum of 11°C, and a precipitation mean of 103. All plots were predicted to increase in both the maximum and minimum temperature, but

the plots in Florida and Georgia were the only two plots with predictions to decrease in average precipitation between the 2070-2095 time period and the 2006-2031 time period (Table 3).

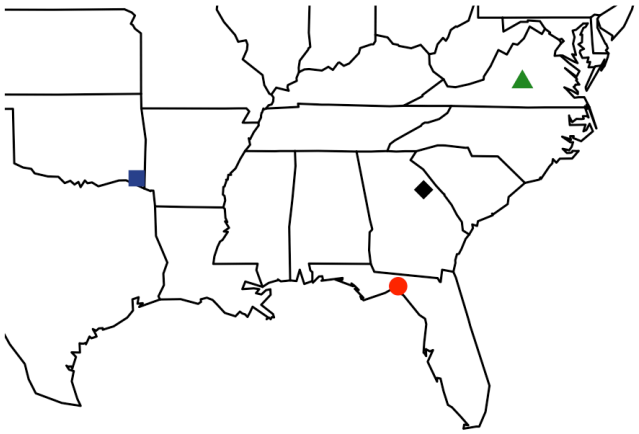

***Figure 4**: Sites selected for analysis. Blue square is Oklahoma plot, red circle is Florida plot, black diamond is Georgia plot, and green triangle is Virginia plot*

Table 3: Predicted change in climate between mean of 2070-2095 and mean of 2006-2031 at each site. Negative signifies a negative change, or a decrease.

	VA	FL	OK	GA
Change in Temp Max (Mean, °C)	3.63	3.15	3.80	3.34
Standard Deviation	2.62	1.73	2.32	2.15
Change in Temp Min (Mean, °C)	3.64	2.98	3.66	3.18
Standard Deviation	4.00	2.54	3.37	3.08
Change in Precipitation (Mean, %change)	5.25	-2.36	-4.44	2.69
Standard Deviation	7.02	9.80	10.41	8.21

We ran each simulation for 25 years, which is the average age of harvesting for loblolly pine plantations. We ran simulations for a stand planted in year 2006 (growing until year 2031) and a stand planted in 2070 (growing until year 2095). These were paired simulations; the same parameters were selected for each simulation, with only the climate data altered depending on the selected year. We calculated total biomass levels, standard deviation, and medians of each prediction at age 25. We used the standard deviation as an indication of the magnitude of uncertainty in our predictions (Hastings 1970). Each plot incorporated specific site information

and climate data for the specified latitude and longitude. We calculated a probability distribution for the difference in biomass between the two stands at age 25, and we used that distribution of change in total biomass to calculate the standard deviation (uncertainty in the prediction) and the median change (average amount of expected change in biomass) for each plot. Since these were paired simulations, the differences were also paired in order to reduce uncertainty. We also used the distribution to calculate the probability of an increase in biomass by calculating the area under the curve for all values greater than zero. This probability represented the probability of a positive difference between the 2006 stand and the 2070 stand at age 25. A positive difference between the two stands meant an increase in biomass accumulation at that plot.

Chapter 4: Results

4.1 Predictions of Biomass by Plot

Biomass is expected to increase over time in plots planted in 2070 compared to plots planted in 2006 under RCP 8.5 for all four sites when all forms of uncertainty were incorporated (Figure 5). The credible intervals when all uncertainty was incorporated for plots planted in 2070 showed potential values of higher biomass accumulation than the credible intervals for those in 2006, with 2070 also showing a wider possible range of values than the 2006 plots. However, there was variation among the sites, with Virginia demonstrating the largest difference and the least overlap of credible intervals between plots planted in 2006 and 2070. Results using RCP 4.5 had similar patters with a lower amount of overall biomass change for all sites (Figure 6).

In addition, comparisons between the two stands at age 25 using the median value showed consistent increase in total biomass accumulation over time. The consistently positive median values at all sites quantify the extent of the increase in biomass at each site (Table 4). We additionally compared probability distributions for the difference between the 2070 stands and the 2006 stands (Figure 7). Overall all sites had a 50% or greater probability of increased biomass between stands planted in 2006 and those planted in 2070 for both RCP 8.5 and RCP 4.5 (Table 5).

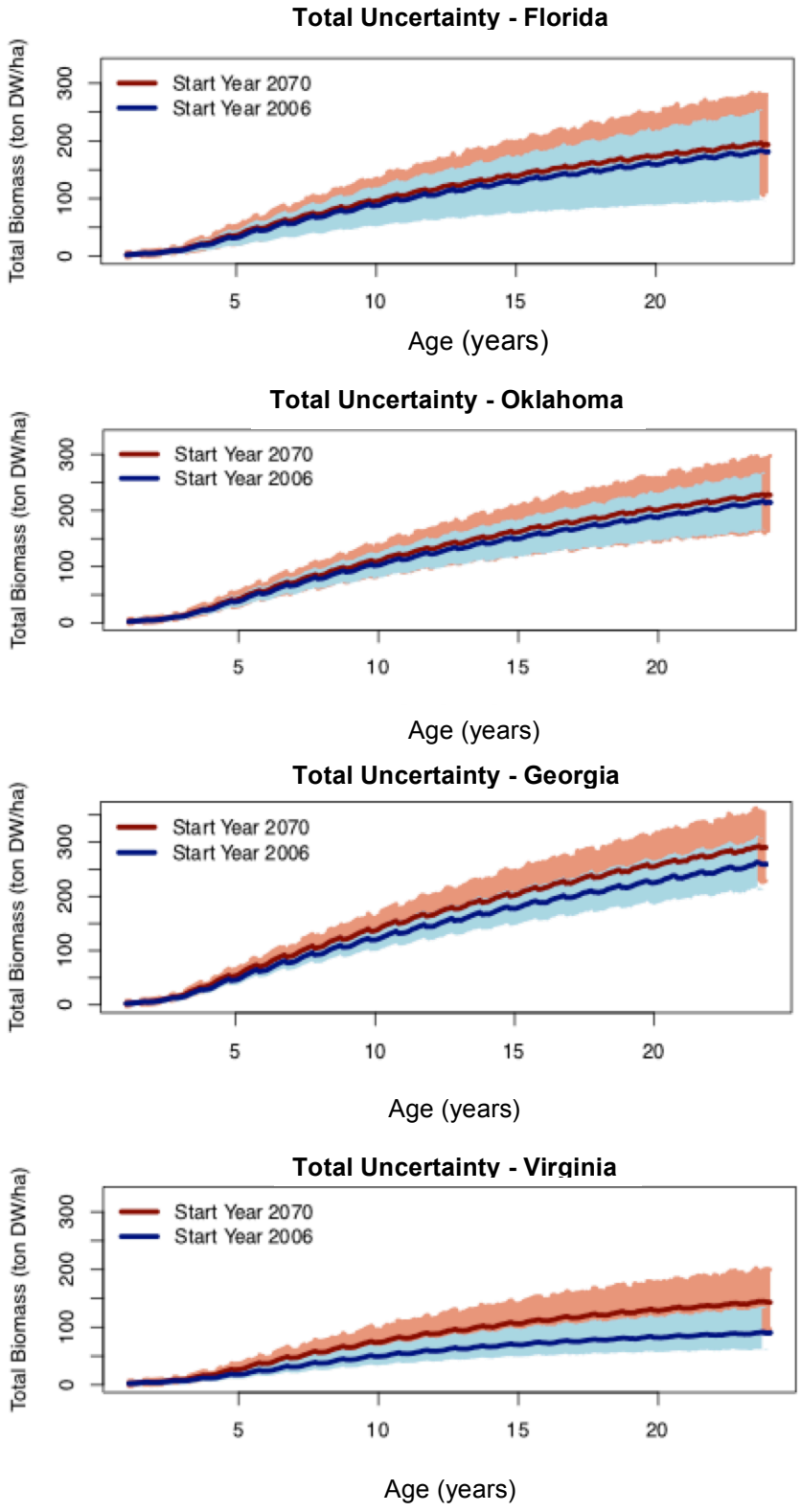

Figure 5: *Total predicted biomass accumulation over 25 years at a single plot, for two stands. One stand planted in 2006 (blue line and shading for 95% credible interval) and one stand planted in 2070 (red line and shading for 95% credible interval). Run with RCP 8.5, with all forms of uncertainty incorporated.*

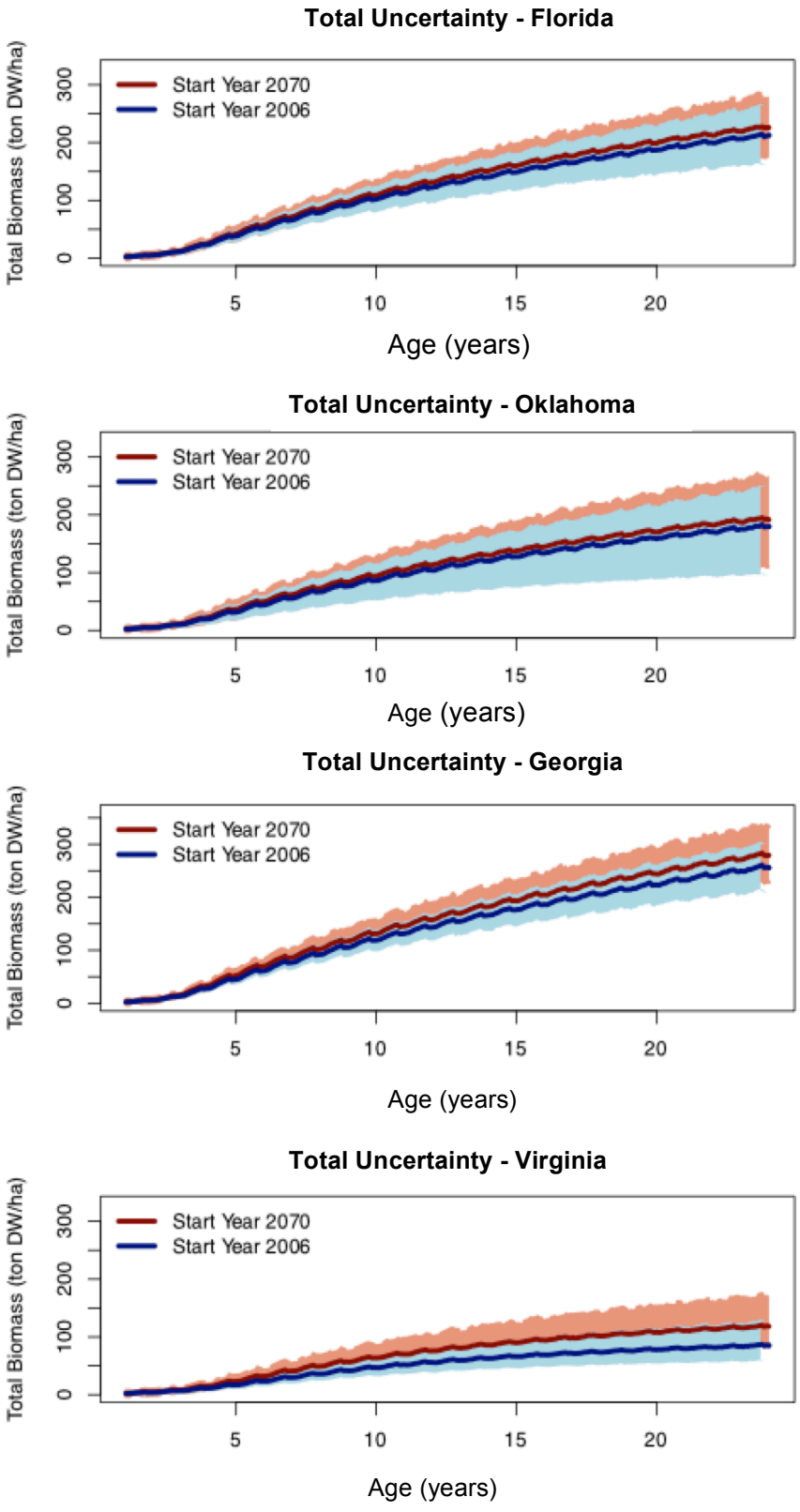

Figure 6: *Total predicted biomass accumulation over 25 years at a single plot, for two stands. One stand planted in 2006 (blue line and shading for 95% credible interval) and one stand planted in 2070 (red line and shading for 95% credible interval). Run with RCP 4.5, with all forms of uncertainty incorporated.*

Table 4: Median difference in biomass at each site, between a plot planted in 2070 and a plot planted in 2006 using RCP 8.5. Median represents the average predicted change in biomass accumulation over 65 years at that site. Since they are all positive, all sites predict an average increase in biomass of these median values. Process Model Uncertainty and Climate Model Uncertainty are averaged across climate models; see all individual values in supplemental material (Ton DW/ha).

Uncertainty Incorporated	VA	FL	OK	GA
Process Model Uncertainty	53.03	13.36	15.66	31.87
Parameter Uncertainty	52.56	11.95	12.79	32.60
Climate Model Uncertainty	57.49	18.25	12.67	33.45
All Three – Overall Prediction	51.36	12.23	14.72	31.83

Table 5: Probability of any increase in biomass at each site

Scenario Incorporated	VA	FL	OK	GA
RCP 8.5	96%	62%	60%	79%
RCP 4.5	89%	64%	59%	76%

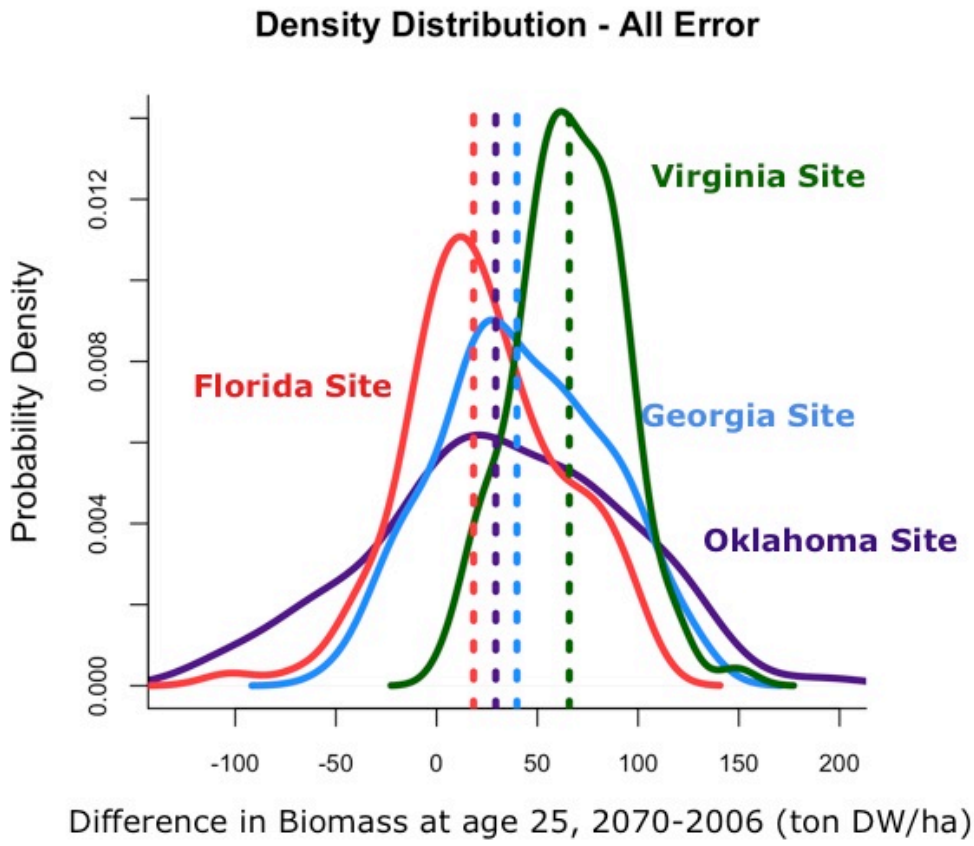

Figure 7: *Probability distributions of the difference between the 2070 and the 2006 stands at each plot at age 25. Dotted lines show the median value for the distribution. Demonstrates the range of uncertainty for each site and difference in potential increase in biomass.*

The results shown in Table 4 for process and parameter uncertainty were averaged across climate models, but it is important to note that there was wide variation between the individual climate models used for the distributions produced for both process and parameter uncertainty predictions (Appendix B). The sites with the greatest variation were Oklahoma and Florida, and Virginia was the site with the most consistent predictions across climate model incorporation (meaning the Virginia results showed the least differences in predicted results between the different climate models). For example, in Oklahoma for RCP 8.5 with model only incorporated we saw a maximum median prediction of 51.73 Ton DW/ha and a minimum predicted median difference of -21.06 Ton DW/ha (which averaged out to 15.55 Ton DW/ha). In contrast, for Virginia with RCP 8.5 the maximum median with model error incorporation was 74.89 Ton DW/ha, and the minimum was 27.20 Ton DW/ha. However, there was less variation between models for those simulated with RCP 4.5 than those with RCP 8.5. In contrast to the earlier example, in Oklahoma for RCP 4.5 with model only incorporated the maximum median prediction was 36.96 Ton DW/ha, and the minimum was only -7.68 Ton DW/ha.

To analyze the sensitivity of biomass predictions to CO_2 fertilization, we simulated a plot with the same climate change effects across models with RCP 8.5, but with CO_2 levels held constant at 2006 ppm. The resulting predictions had a higher level of certainty predicting a decrease in biomass with the effects of climate change (Figure 8). The median change in aboveground biomass at age 25 between years 2006 and 2070 with the CO2 held constant was consistently below zero with -2.20 ton DW/ha in Virginia, -26.94 ton DW/ha in Florida, -32.39 ton DW/ha in Oklahoma, and -26.34 ton DW/ha in Georgia. The standard deviation for those predictions was 21.532 ton DW/ha in Virginia, 37.937 ton DW/ha in Florida, 55.268 ton DW/ha in Oklahoma, and 30.672 ton DW/ha in Georgia.

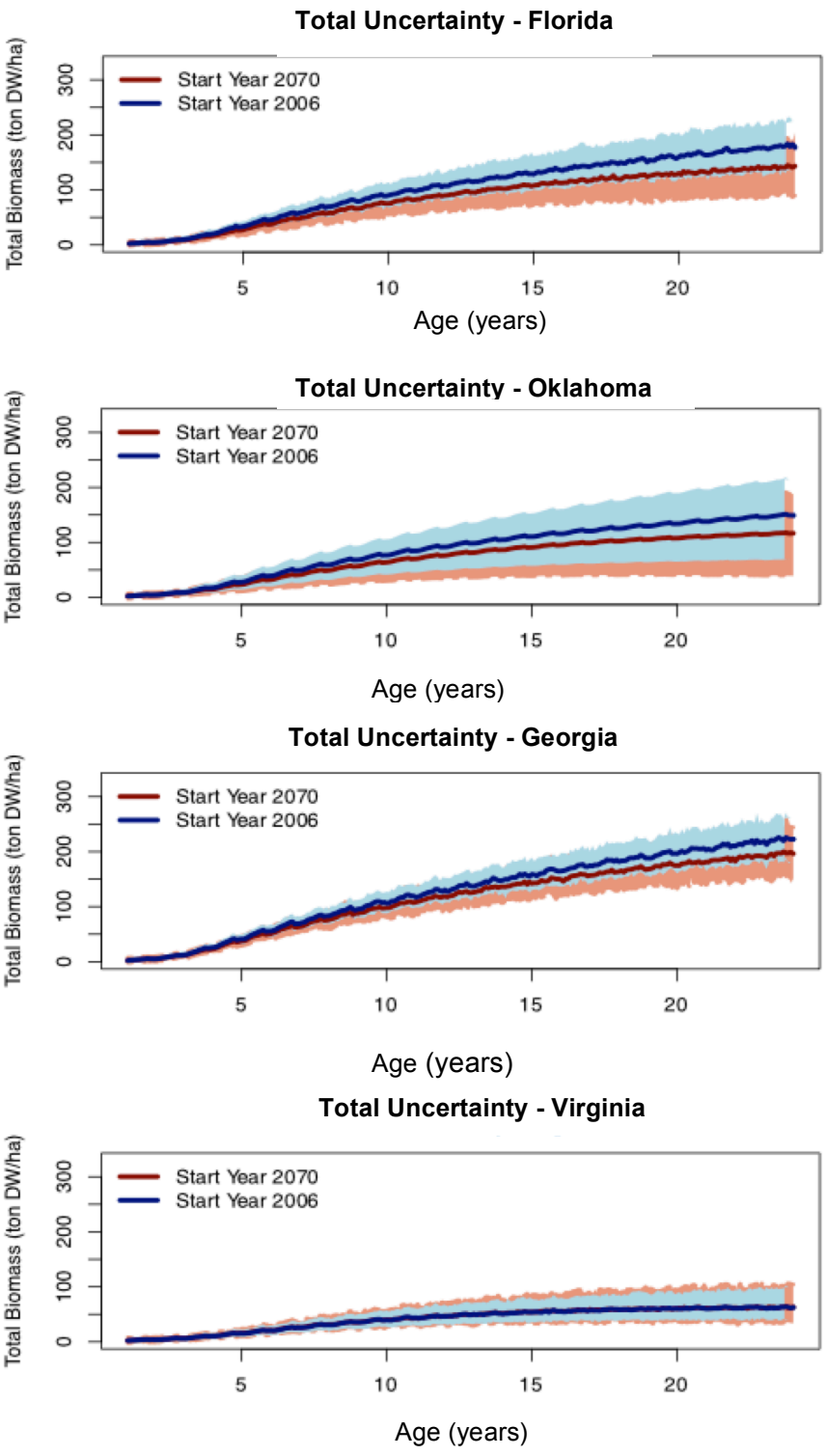

Figure 8: *Total predicted biomass accumulation over 25 years at a single plot, for two stands. One stand planted in 2006 (blue line and shading for 95% credible interval) and one stand planted in 2070 (red line and shading for 95% credible interval). Simulation of CO_2 fertilization effect with CO_2 values held constant at 2006 levels while climate predictions maintained RCP 8.5 predictions.*

4.2 The Role of Uncertainty in Predictions

Comparisons of standard deviation showed that process and parameter uncertainty had the largest influence on the overall uncertainty in a prediction. To analyze the change in impact of uncertainty with different emission scenarios, RCP 4.5 and RCP 8.5 were run for each site with each uncertainty type. RCP 4.5 maintained similar levels of uncertainty for ecosystem model parameter and process uncertainty, but had a much lower standard deviation climate model uncertainty (Table 6). Standard deviation comparisons between predictions for RCP 4.5 and RCP 8.5 showed a decrease in total uncertainty across all four sites when the lower emissions scenario was employed (Table 6). Comparisons made of the standard deviation when simulating the removal of CO_2 fertilization showed a decrease in uncertainty as well.

Table 6: Standard Deviation of the difference in biomass between year 2006 and year 2070 at age 25. Standard deviation represents the amount of uncertainty for each prediction at each site. Standard Deviation for ecosystem model process and parameter is averaged across all 20 climate models. (ton DW/ha)

Uncertainty Incorporated	VA		FL		OK		GA	
RCP Used	**4.5**	**8.5**	**4.5**	**8.5**	**4.5**	**8.5**	**4.5**	**8.5**
Process	12.29	13.68	26.22	25.3	22.51	22.23	32.77	33.48
Model Parameter	22.20	23.00	26.89	28.2	50.61	59.52	10.46	13.57
Climate Model	7.42	13.94	5.06	18.08	9.61	17.66	7.59	16.61
All Three	27.07	30.20	38.11	41.79	57.26	59.48	33.78	38.41

Chapter 5: Discussion

Overall, there was a high probability (>59%) of increase in biomass accumulation over time in the four sites analyzed with all uncertainty incorporated. Therefore, based on our modeling analysis, the effect of climate change and rising atmospheric CO_2 is likely to have a positive impact on loblolly pine growth in southeast U.S. loblolly pine plantations, increasing the amount of carbon stored in vegetation at each plot. However, this biomass accumulation varied regionally, with the most Northern and coolest site (Virginia) predicted to see the largest amount of change in biomass accumulation over time. Comparing the three types of uncertainty (climate model, ecosystem model process, and ecosystem model parameter), the ecosystem model

uncertainty associated with the parameters and the process model were a greater influence on predictions than the climate model uncertainty. Uncertainty levels varied regionally as well, with Oklahoma as the site with the most uncertainty associated with predictions and Virginia as the least uncertain.

Although we overall saw a predicted increase in biomass across the region, there was variation in the amounts of biomass increase predicted between the sites. Virginia, the most Northern of the sites, had the highest probability of an increase in biomass. The two most southern and western sites on the edge of the loblolly range, Oklahoma and Florida, had the lowest probability of increase and the least amount of predicted increase in biomass accumulation. The environmental modifiers that influence the light use efficiency in the 3-PG model provide a basis for analyzing the environmental drivers of the variation among the plots (see Introduction) (Figure 9). In our study, these environmental modifiers in 3-PG were calibrated to the region-wide observations of biomass growth and monthly GEP from the two loblolly pine flux towers. Other studies have shown the environmental modifiers to accurately simulate loblolly pine response behavior (Landsberg et al. 2001).

The most important driver of change in light use efficiency (LUE) and biomass growth was an increase in atmospheric CO_2. The atmospheric CO_2 modifier (figure 9b) showed the largest change of the set of environmental modifiers between the stand planted in 2006 and the stand planted in 2070. The increase in light use efficiency was the same across all sites because the atmospheric CO_2, a gas that is well mixed in the atmosphere, was assumed constant across the region. The RCP scenarios predict an increase in CO_2 levels between the stands planted in 2006 and 2070, and a larger increase when the RCP 8.5 scenario is used instead of the lower-emission scenarios. This increase in influence of CO_2 on the stand light use efficiency can greatly impact overall biomass accumulation. An elevated level of CO_2 in the atmosphere can cause partial closure of stomata and allow reduced transpiration, increasing plant water usage efficiency and diminishing the decline of soil moisture (Wullschleger et al. 2002). The sensitivity analysis we conducted on CO_2 fertilization showed that isolating CO_2 from the other effects of climate change caused a decrease in biomass because the change in the other environmental modifiers was either a relatively small increase or a decrease over the 21st century. Overall, the small increases in biomass in Georgia, Florida, and Oklahoma sites are due to the balance of CO_2 increasing LUE and the net influence of the other modifiers decreasing growth (temperature,

VPD, frost days, and soil water). The larger increase at the Virginia site was due to the net influences of the other non-CO2 environmental modifiers being more positive than the other three sites.

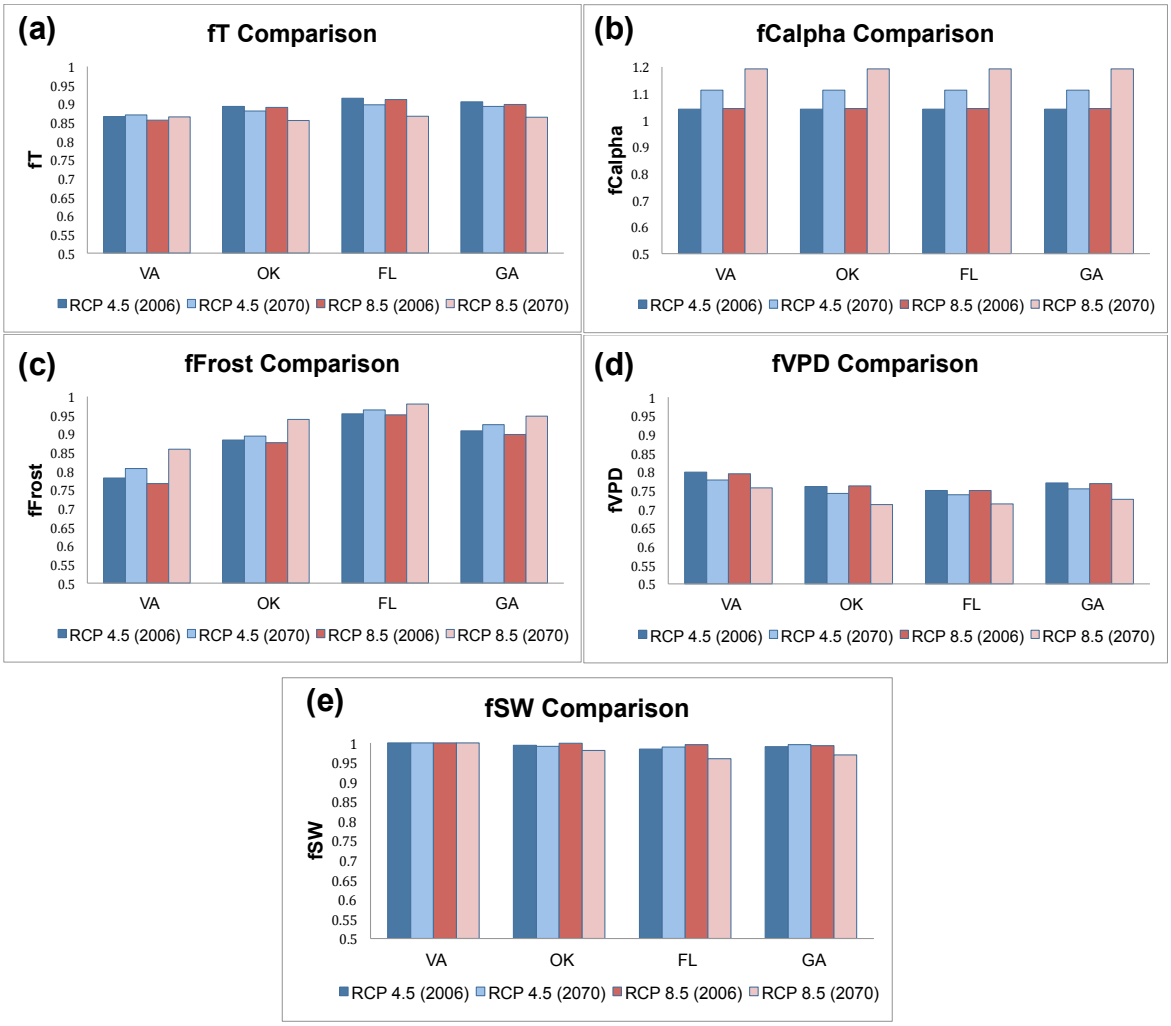

***Figure 9**: Environmental Modifiers from the 3-PG Model for each site. Values are averaged across each growing period (2006-2031, 2070-2095), run with each RCP climate scenario. Each modifier shows the average value for that selected growing period for each site; the greater the change in the modifier, the greater the impact of that modifier on the growth at that site. Larger values correspond to greater light use efficiency.*

Of the non-CO_2 environmental modifiers, the most important driver of change was a decrease in frost days. The frost modifier varies regionally, resulting in a different level of impact depending on the climate change predictions at each of the four sites. The Virginia site

has the largest amount of change with a median of 51.37 ton DW/ha for RCP 8.5, showing a clear impact of the decrease in the amount of frost days. This decrease in frost days increases light use efficiency and tree growth in the 3-PG model with a value of 1 for this modifier corresponding to a month with frost days. All four sites consistently were predicted to have a decrease in frost days between the 2006 and the 2070 stands, but Florida has the least amount of change, contributing to the least amount of change in predicted biomass. Frost days can affect loblolly pine by changing the length of the growing season, which has a big impact on the amount of growth at a site (McMurtrie et al. 1994). Variation in the frost-free season during which the seed originated, and the duration of the seasonal growth period (amount of frost-free days) accounts for about 30% of total height growth variation in plantations (Perry et al. 1966). However, the frost day modifier does not take into account disturbances such as unexpected frost events that can impact bud production and yearly growth for a plantation.

The last two influential environmental drivers of change were the vapor pressure deficit and the temperature response modifiers. The impact on light use efficiency is calculated from the minimum of either VPD or soil moisture, and in all cases the VPD modifier is lower than the soil moisture modifier. Therefore, the influences of the water cycle on LUE and biomass growth were driven entirely by increases in VPD over time. Virginia and Georgia have the least change for RCP 8.5 in VPD between a stand planted in 2006 and 2070, while Oklahoma and Florida experience slightly larger changes. As trees absorb the CO_2 required for photosynthesis, they also transpire and lose water through their stomata. A higher vapor pressure deficit, which can be caused by hotter and drier conditions, increases the rate of transpiration and can decrease the efficiency of a plant. The change in VPD in the model simulations was driven by an increase in temperature, as relative humidity is not used as an input to the model. The VPD response represents an interaction between temperature and VPD that can result in higher transpiration, more negative xylem water potentials, and a quicker reduction in leaf gas exchange. For example, studies of seedlings grown along the forest-grassland ecotone, which include sites such as Oklahoma that are on the edge of the moisture limit of the native range of loblolly pine, were subjected to increased temperature and decreased precipitation which killed seedlings 13% sooner with only a 3°C change (Will et al. 2013). Because soil moisture modifier was always less than the VPD modifier, the small reductions in the soil moisture modified in Figure 7e did

not influence LUE and biomass growth. By lacking an influence of soil on growth, the simulations may not include a known driver of loblolly growth rates.

Beyond the indirect influence of increased temperature on LUE and biomass growth through increases in VPD, increased temperature has a direct influence on changes in LUE and biomass growth over the 21st century. Although temperature response was smaller than the VPD response, it was the only modifier that differs in sign depending on location in the region. Although Georgia also sees a decrease in fT (meaning an increased impact of fT on growth), Florida and Oklahoma have the largest change in fT between the two plots. The northern portion of the loblolly pine native range is expected to have overall larger increases in precipitation with the effects of climate change, and Florida and Oklahoma are the only sites that predicted a likely decrease in precipitation over time. Similarly, all portions of the United States will experience an increase in temperature. Sites like Florida which are already at the upper limits of the loblolly range (in 2015 had an average maximum temperature of 27°C and a July temperature of 34°C), could experience around a 3-degree increase in temperature bringing their average yearly maximum temperature to 30°C and a July high of 37°C. Loblolly pines optimum temperature range is between 25°C to 30°C, with an average July temperature of 27°C, and with survival but decreased biomass accumulation at 35°C and only 14% of seedlings surviving temperatures at 40°C (Teskey and Will 1999). This change in temperature could bring the Florida site very close to or above the optimal temperature range for the trees. In comparison, the Virginia site had an average maximum temperature of 20°C and a July temperature of 31.2°C in 2015. A potential change of about 3.6°C pushes the average yearly max to 23°C and a July temperature of 34.2°C. In contrast to Florida, this increase in temperature in Virginia is pushing the site closer to the optimum value for loblolly pines.

Overall, our findings reflect general predictions that the warmest regions of the loblolly pine native range are expected to be more vulnerable to changes in productivity and hydrology than forests located in wetter and cooler areas (McNulty et al. 1996). Supporting our findings are regional variation patterns that have been observed across Europe, where the northern forests are predicted to have a greater increase of carbon storage due to an increased growing season in comparison to areas of southern Europe which are more dominated by changing water balance (Olesen et al. 2007). In addition, studies have found that with CO_2 fertilization, a cool site (-2°C ambient temperature) experienced stimulated biomass accumulation of 38% and a warm site

(+2°C ambient temperature) experienced only a 24% stimulated biomass accumulation (Wertin et al. 2012). Increased precipitation often correlates with an increase in forest carbon sequestration, and higher air temperatures can result in lower storage of carbon (Lu et al. 2015). Although the overpowering positive influence of CO_2 fertilization results in predictions for an increase in biomass over time across the loblolly range (DeLucia et al. 1999, Schlesinger et al. 2006), understanding the effects of the environmental modifiers in the model can help to explain regional differences in prediction biomass and uncertainty.

While all sites predicted an increase in biomass over the 21st century due to climate change and increasing atmospheric CO2, there was considerable uncertainty in predictions. We found that the primary drivers of uncertainty were uncertainty in ecosystem model parameters and uncertainty in ecosystem model structure (process uncertainty). While a complete examination of all parameters that contribute to the parameter uncertainty was not performed, we found that the parameter that controlled the LUE response to atmospheric CO_2 strongly influenced the magnitude of uncertainty. Uncertainty in the impact of increasing CO_2 on loblolly pine plantations is partially due to limited number of sites that measured whole-ecosystem responses to elevated CO_2 and the lack of research done at extremely high levels of atmospheric CO_2. Studies like Duke FACE have tested elevated levels up to 590 ppm (Schlesinger et al. 2006), but there have been none testing levels at the RCP 8.5 scenario which predicts closer to 900 ppm by the end of the century. For this reason an increase in research to reduce uncertainty in CO_2 response parameterization is important for improving accuracy of predictions.

The uncertainty from the ecosystem model remained the most dominant with both RCP emission scenarios, meaning that the ecosystem model uncertainty was a larger impact than the climate model uncertainty no matter what human actions and mitigation are assumed. With a lower RCP emission scenario, we saw a large reduction in climate model uncertainty because the climate models had higher agreement for future climate. While climate models offer a wide range of possible climate results, sometimes with different signs of predictions for future climate, our findings suggest that focusing more on reducing uncertainty in parameter or process model could result in lower overall uncertainty in ecosystem predictions.

In addition, we calculated variation in the uncertainty between sites and between climate models at a single site. The Oklahoma site had the most uncertainty, driven primarily by ecosystem model parameter uncertainty. The Georgia site had the most process model

uncertainty, and the Virginia site (the most Northern location of all the sites) had the least amount of uncertainty associated with predictions. We saw some correlation between higher levels of parameter uncertainty and lower predictions of biomass increase. The sites that have larger amounts of change in the environmental modifiers of vapor pressure deficit and temperature also had more uncertainty in how much these modifiers would affect the overall growth of the stand. This shows that certain environmental modifiers such as those associated with hydrology and soil moisture could be the least constrained and contribute to higher levels of uncertainty in the impact on forest growth. For these reasons, increased research constraining the loblolly parameters affecting these environmental modifiers could result in the most efficient reduction of uncertainty for these predictions.

Data assimilation as a technique allows for better model predictions with a more robustly quantified uncertainty, and with data assimilation our results contributed to the improvement of ecological forecasting and quantification of uncertainty estimates. Many studies have used data assimilation and the MHMCMC technique to improve predictions on carbon storage (van Oijen et al. 2005, Xu et al. 2006, Weng and Luo 2011, Sus et al. 2013). However, what has largely been absent in current studies is a full quantification of all forms of uncertainty in forecasts, specifically for loblolly pines in the Southeast U.S. Identifying the primary source of uncertainty within these predictions is important to make improvements on future forecasts and accurately identify the areas that need the most focus in future research. Although our research does not necessarily capture every possible form of uncertainty and there are some uncertainties not discussed in this study, identifying several large impacts of uncertainty and comparing them can help to improve recommendations for future research. Using the data assimilation to improve results lends to more accurate predictions overall.

Our predictions that biomass will increase over the 21st century in loblolly pine plantations of the southeastern U.S. includes the influences of CO2, temperature, frost days, and VPD changes but does not include changes to the regional disturbance regime or management practices. We incorporate data and analyze the carbon sink uncertainty for forest age and land management, but the analysis is missing the crucial effect of disturbances (other than regular, planned harvests), which could have a significant impact on the carbon storage predictions. For example, disturbances such as pest infestation or wind and hurricane events can have a large effect on ecophysiological function and growth of loblolly pines (Kelley and King 2014).

Additional disturbances such as heat waves and drought can also have implications, as many studies and climate models measure a slow change of temperature over time and few study the response of forests to a highly elevated temperature over a short period of time (Ameye et al. 2012). For these reasons, we recommend future research incorporating disturbances into the ecosystem model.

This research is important for the loblolly pine plantation industry by creating more accurate predictions allowing proper mitigation, management, and planning. Identifying the probability of increased biomass accumulation, predicting future carbon sequestration in stands, and quantifying the uncertainty in those predictions could be critical for both management decisions and potential improvement in C credits for landowners by allowing for better informed decisions (Johnsen et al. 2004). With the international focus increasing on climate change mitigation and carbon storage possibilities, there has been increased interest in the carbon storage potential for industrial plantation owners. Accounting for the scientific uncertainty and providing increased information about predictions of carbon storage in plantations can allow plantation owners and forest managers to improve the ecological benefits of their management decisions. This in turn will contribute to the economic and ecological prospects for the plantations (Brown et al. 2006). There have been several calls for increased quantification of uncertainty and use of mathematical methods in ecosystem analysis in order to improve quantification of predictions made for terrestrial ecosystems (Hobbs and Ogle 2011, Keenan et al. 2011), and identifying the areas of uncertainty that can make the biggest influence on forest ecosystem predictions are critical, both in focusing future research on field studies and in model development that will reduce prediction uncertainty.

In conclusion, our results showed the importance of incorporating and analyzing uncertainty into the predictions of aboveground biomass and carbon storage in loblolly pine plantations. When only evaluating the average median values, all results show a positive change in aboveground biomass between years 2006 and 2070. None of the medians accurately represent the uncertainty associated with that prediction, which can actually lead to the possibility of an opposite, decrease in biomass. In addition, we found the greatest influence on uncertainty to be parameter and process model uncertainty. Although climate models have offered a wide variation in predicted results and were initially expected to have a more significant influence on predictions, it was shown that the greater uncertainty was coming from process model and

parameter uncertainty. Finally, we found that the biomass and uncertainty predictions are extremely sensitive to CO_2 fertilization, and this could be one of the primary drivers of increased uncertainty levels and increased biomass accumulation in loblolly pine forests. These conclusions lead to important future research goals and an ability to focus research on uncertainty sources that will yield the greatest results in achieving accurate predictions in the future.

References

Abatzoglou, J. T. 2013. Development of gridded surface meteorological data for ecological applications and modelling. International Journal of Climatology 33:121–131.

Ameye, M., T. M. Wertin, I. Bauweraerts, M. A. McGuire, R. O. Teskey, and K. Steppe. 2012. The effect of induced heat waves on Pinus taedaand Quercus rubraseedlings in ambient and elevated CO 2atmospheres. New Phytologist 196:448–461.

Ascough, J. C., II, H. R. Maier, J. K. Ravalico, and M. W. Strudley. 2008. Future research challenges for incorporation of uncertainty in environmental and ecological decision-making. Ecological Modelling 219:383–399.

Bellouin, N., O. Boucher, J. Haywood, C. Johnson, A. Jones, J. Rae, and S. Woodward. 2007. Improved representation of aerosols for HadGEM2. Hadley Centre Tech.

Bentsen, M., I. Bethke, J. B. Debernard, T. Iversen, A. Kirkevåg, Ø. Seland, H. Drange, C. Roelandt, I. A. Seierstad, C. Hoose, and J. E. Kristjánsson. 2013. The Norwegian Earth System Model, NorESM1-M – Part 1: Description and basic evaluation of the physical climate. Geoscientific Model Development 6:687–720.

Bloom, A. A., and M. Williams. 2015. Constraining ecosystem carbon dynamics in a data-limited world: integrating ecological "common sense" in a model–data fusion framework. Biogeosciences 12:1299–1315.

Bonan, G. B. 2008. Forests and Climate Change: Forcings, Feedbacks, and the Climate Benefits of Forests. Science 320:1444–1449.

Brown, S., E. Palola, and M. Lorenzo. 2006. The possibility of plantations: Integrating ecological forestry into plantation systems.

Bryars, C., C. Maier, D. Zhao, M. Kane, B. Borders, R. Will, and R. Teskey. 2013. Fixed physiological parameters in the 3-PG model produced accurate estimates of loblolly pine growth on sites in different geographic regions. Forest Ecology and Management 289:501–514.

Canadell, J. G., C. Le Quéré, M. R. Raupach, C. B. Field, E. T. Buitenhuis, P. Ciais, T. J. Conway, N. P. Gillett, R. A. Houghton, and G. Marland. 2007. Contributions to accelerating atmospheric CO2 growth from economic activity, carbon intensity, and efficiency of natural sinks. Proceedings of the National Academy of Sciences 104:18866–18870.

Chylek, P., J. Li, M. K. Dubey, M. Wang, and G. Lesins. 2011. Observed and model simulated 20th century Arctic temperature variability: Canadian Earth System Model CanESM2. Atmospheric Chemistry and Physics Discussions 11:22893–22907.

Clark, J. S., and A. E. Gelfand. 2006. A future for models and data in environmental science. Trends in Ecology & Evolution 21:375–380.

Coops, N. 1999. Improvement in predicting stand growth of Pinus radiata (D. Don) across landscapes using NOAA AVHRR and Landsat MSS AVHRR and Landsat MSS imagery combined with a forest growth process model (3-PGS). Photogrammetric engineering and remote sensing.

Coops, N. C., and R. H. Waring. 2001. Assessing forest growth across southwestern Oregon under a range of current and future global change scenarios using a process model, 3‐PG. Global Change Biology 7:15–29.

Cramer, W., A. Bondeau, and F. I. Woodward. 2001. Global response of terrestrial ecosystem structure and function to CO2 and climate change: results from six dynamic global vegetation models. Global change Biology 7:357–373.

DeLucia, E. H., J. G. Hamilton, S. L. Naidu, R. B. Thomas, J. A. Andrews, A. Finzi, M. Lavine, R. Matamala, J. E. Mohan, G. R. Hendrey, and W. H. Schlesinger. 1999. Net Primary Production of a Forest Ecosystem with Experimental CO2 Enrichment. Science 284:1177–1179.

Dietze, M. C., D. S. LEBAUER, and R. KOOPER. 2013. On improving the communication between models and data. Plant, Cell & Environment 36:1575–1585.

Dufresne, J. L., M. A. Foujols, S. Denvil, A. Caubel, O. Marti, O. Aumont, Y. Balkanski, S. Bekki, H. Bellenger, R. Benshila, S. Bony, L. Bopp, P. Braconnot, P. Brockmann, P. Cadule, F. Cheruy, F. Codron, A. Cozic, D. Cugnet, N. de Noblet, J. P. Duvel, C. Ethé, L. Fairhead, T. Fichefet, S. Flavoni, P. Friedlingstein, J. Y. Grandpeix, L. Guez, E. Guilyardi, D. Hauglustaine, F. Hourdin, A. Idelkadi, J. Ghattas, S. Joussaume, M. Kageyama, G. Krinner, S. Labetoulle, A. Lahellec, M. P. Lefebvre, F. Lefevre, C. Levy, Z. X. Li, J. Lloyd, F. Lott, G. Madec, M. Mancip, M. Marchand, S. Masson, Y. Meurdesoif, J. Mignot, I. Musat, S. Parouty, J. Polcher, C. Rio, M. Schulz, D. Swingedouw, S. Szopa, C. Talandier, P. Terray, N. Viovy, and N. Vuichard. 2013. Climate change projections using the IPSL-CM5 Earth System Model: from CMIP3 to CMIP5. Climate Dynamics 40:2123–2165.

Dunne, J. P., J. G. John, A. J. Adcroft, S. M. Griffies, R. W. Hallberg, E. Shevliakova, R. J. Stouffer, W. Cooke, K. A. Dunne, M. J. Harrison, J. P. Krasting, S. L. Malyshev, P. C. D. Milly, P. J. Phillipps, L. T. Sentman, B. L. Samuels, M. J. Spelman, M. Winton, A. T. Wittenberg, and N. Zadeh. 2012. GFDL's ESM2 Global Coupled Climate–Carbon Earth System Models. Part I: Physical Formulation and Baseline Simulation Characteristics. Journal of Climate 25:6646–6665.

Esprey, L. J., P. J. Sands, and C. W. Smith. 2004. Understanding 3-PG using a sensitivity analysis. Forest Ecology and Management 193:235–250.

Feng, G., X. Xiaoge, and W. Tongwen. 2012. Study on the Prediction of Regional and Global Temperature in Decadal Time Scale with BCC CSM1. 1. Chinese Journal of Atmospheric Sciences.

Fox, A., M. Williams, A. D. Richardson, D. Cameron, J. H. Gove, T. Quaife, D. Ricciuto, M. Reichstein, E. Tomelleri, C. M. Trudinger, and M. T. Van Wijk. 2009. The REFLEX project: Comparing different algorithms and implementations for the inversion of a terrestrial ecosystem model against eddy covariance data. Agricultural and Forest Meteorology 149:1597–1615.

Fox, T. R., E. J. Jokela, and H. L. Allen. 2007. The development of pine plantation silviculture in the southern United States. Journal of Forestry.

Gao, C., H. Wang, E. Weng, S. Lakshmivarahan, Y. Zhang, and Y. Luo. 2011. Assimilation of multiple data sets with the ensemble Kalman filter to improve forecasts of forest carbon dynamics. Ecological applications : a publication of the Ecological Society of America 21:1461–1473.

Gardner, R. H., R. V. O'neill, J. B. Mankin, and J. H. Carney. 1981. A comparison of sensitivity analysis and error analysis based on a stream ecosystem model. Ecological Modelling 12:173–190.

Gent, P. R., G. Danabasoglu, L. J. Donner, M. M. Holland, E. C. Hunke, S. R. Jayne, D. M. Lawrence, R. B. Neale, P. J. Rasch, M. Vertenstein, P. H. Worley, Z.-L. Yang, and M. Zhang. 2011. The Community Climate System Model Version 4. Journal of Climate 24:4973–4991.

Hastings, W. K. 1970. Monte Carlo sampling methods using Markov chains and their

applications. Biometrika 57:97–109.
Hill, T. C., M. Williams, F. I. Woodward, and J. B. Moncrieff. 2011. Constraining ecosystem processes from tower fluxes and atmospheric profiles. Ecological applications : a publication of the Ecological Society of America 21:1474–1489.
Hobbs, N. T., and K. Ogle. 2011. Introducing data-model assimilation to students of ecology. Ecological applications : a publication of the Ecological Society of America 21:1537–1545.
Intergovernmental Panel on Climate Change. 2014. Climate Change 2014–Impacts, Adaptation and Vulnerability: Regional Aspects.
Ji, D., L. Wang, J. Feng, Q. Wu, H. Cheng, Q. Zhang, J. Yang, W. Dong, Y. Dai, D. Gong, R. H. Zhang, X. Wang, J. Liu, J. C. Moore, D. Chen, and M. Zhou. 2014. Description and basic evaluation of BNU-ESM version 1. Geoscientific Model Development Discussions 7:1601–1647.
Johnsen, K., B. Teskey, L. Samuelson, J. Butnor, D. Sampson, F. Sanchez, C. Maier, and S. McKeand. 2004. Carbon Sequestration in loblolly pine plantations: Methods, limitations, and research needs for estimating storage pools.
Keenan, T. F., M. S. Carbone, M. Reichstein, and A. D. Richardson. 2011. The model–data fusion pitfall: assuming certainty in an uncertain world. Oecologia 167:587–597.
Kelley, A. M., and J. S. King. 2014. Pest pressure, hurricanes, and genotype interact to strongly impact stem form in young loblolly pine (Pinus taeda L.) along the coastal plain of North Carolina. Trees 28:1343–1353.
Landsberg, J. J., and R. H. Waring. 1997. A generalised model of forest productivity using simplified concepts of radiation-use efficiency, carbon balance and partitioning. Forest Ecology and Management 95:209–228.
Landsberg, J. J., K. H. Johnsen, and T. J. Albaugh. 2001. Applying 3-PG, a simple process-based model designed to produce practical results, to data from loblolly pine experiments. Forest ….
Landsberg, J. J., R. H. Waring, and N. C. Coops. 2003. Performance of the forest productivity model 3-PG applied to a wide range of forest types. Forest Ecology and Management 172:199–214.
Loehle, C., and D. LeBlanc. 1996. Model-based assessments of climate change effects on forests: a critical review. Ecological Modelling 90:1–31.
Lu, X., D. W. Kicklighter, J. M. Melillo, J. M. Reilly, and L. Xu. 2015. Land carbon sequestration within the conterminous United States: Regional- and state-level analyses:1–20.
Luo, Y., E. Weng, X. Wu, C. Gao, X. Zhou, and L. Zhang. 2009. Parameter identifiability, constraint, and equifinality in data assimilation with ecosystem models. Ecological applications : a publication of the Ecological Society of America 19:571–574.
Luo, Y., K. Ogle, C. Tucker, S. Fei, C. Gao, S. LaDeau, J. S. Clark, and D. S. Schimel. 2011. Ecological forecasting and data assimilation in a data-rich era. Ecological applications : a publication of the Ecological Society of America 21:1429–1442.
Mäkelä, A., J. Landsberg, A. R. Ek, T. E. Burk, M. Ter-Mikaelian, G. I. Agren, C. D. Oliver, and P. Puttonen. 2000. Process-based models for forest ecosystem management: current state of the art and challenges for practical implementation. Tree physiology 20:289–298.
McMurtrie, R. E., H. L. Gholz, S. Linder, and S. T. Gower. 1994. Climatic factors controlling the productivity of pine stands: a model-based analysis. Ecological Bulletins.
McNulty, S. G., J. M. Vose, and W. T. Swank. 1996. Potential climate change effects on loblolly

pine forest productivity and drainage across the southern United States. Ambio.
Mélia, D. S. 2002. A global coupled sea ice–ocean model. Ocean Modelling 4:137–172.
Mohren, G., and H. E. Burkhart. 1991. Contrasts between Biologically-based Process Models and Management-oriented Growth and Yield Models. For. Ecol. Manage.
Morales, P., M. T. Sykes, I. C. Prentice, P. Smith, B. Smith, H. Bugmann, B. Zierl, P. Friedlingstein, N. Viovy, S. Sabate, A. Sanchez, E. Pla, C. A. Gracia, S. Sitch, A. Arneth, and J. Ogee. 2005. Comparing and evaluating process-based ecosystem model predictions of carbon and water fluxes in major European forest biomes. Global Change Biology 11:2211–2233.
Murphy, J. M., D. Sexton, D. N. Barnett, and G. S. Jones. 2004. Quantification of modelling uncertainties in a large ensemble of climate change simulations. Nature.
Nakicenovic, N., J. Alcamo, G. Davis, and B. De Vries. 2000. Special report on emissions scenarios, working group III, Intergovernmental Panel on Climate Change (IPCC). Cambridge University Press.
Niu, S., Y. Luo, M. C. Dietze, T. F. Keenan, Z. Shi, J. Li, and F. S. C. III. 2014. The role of data assimilation in predictive ecology. Ecosphere 5:art65–16.
Ogle, K., and J. J. Barber. 2008. Bayesian Data—Model Integration in Plant Physiological and Ecosystem Ecology. Pages 281–311 *in* Progress in Botany. Springer Berlin Heidelberg, Berlin, Heidelberg.
Olesen, J. E., T. R. Carter, C. H. Díaz-Ambrona, S. Fronzek, T. Heidmann, T. Hickler, T. Holt, M. I. Minguez, P. Morales, J. P. Palutikof, M. Quemada, M. Ruiz-Ramos, G. H. Rubæk, F. Sau, B. Smith, and M. T. Sykes. 2007. Uncertainties in projected impacts of climate change on European agriculture and terrestrial ecosystems based on scenarios from regional climate models. Climatic Change 81:123–143.
Pan, Y., R. A. Birdsey, J. Fang, R. Houghton, P. E. Kauppi, W. A. Kurz, O. L. Phillips, A. Shvidenko, S. L. Lewis, J. G. Canadell, P. Ciais, R. B. Jackson, S. W. Pacala, A. D. McGuire, S. Piao, A. Rautiainen, S. Sitch, and D. Hayes. 2011. A Large and Persistent Carbon Sink in the World's Forests. Science 333:988–993.
Perry, T. O., W. Chi-Wu, and D. Schmitt. 1966. Height growth for loblolly pine provenances in relation to photoperiod and growing season. Silvae Genet.
Pinjuv, G., E. G. Mason, and M. Watt. 2006. Quantitative validation and comparison of a range of forest growth model types. Forest Ecology and Management 236:37–46.
Qian, S. S., C. A. Stow, and M. E. Borsuk. 2003. On monte carlo methods for Bayesian inference. Ecological Modelling 159:269–277.
Randall, D. A., and R. A. Wood. 2007. Climate models and their evaluation. Cambridge University Press.
Rotstayn, L. D., S. J. Jeffrey, M. A. Collier, S. M. Dravitzki, A. C. Hirst, J. I. Syktus, and K. K. Wong. 2012. Aerosol- and greenhouse gas-induced changes in summer rainfall and circulation in the Australasian region: a study using single-forcing climate simulations. Atmospheric Chemistry and Physics 12:6377–6404.
Santaren, D., P. Peylin, C. Bacour, P. Ciais, and B. Longdoz. 2014. Ecosystem model optimization using in situ flux observations: benefit of Monte Carlo versus variational schemes and analyses of the year-to-year model performances. Biogeosciences 11:7137–7158.
Schlesinger, W. H., E. S. Bernhardt, E. H. DeLucia, D. S. Ellsworth, A. C. Finzi, G. R. Hendrey, K. S. Hofmockel, J. Lichter, R. Matamala, D. Moore, R. Oren, J. S. Pippen, and R. B.

Thomas. 2006. The Duke Forest FACE Experiment: CO2 Enrichment of a Loblolly Pine Forest. Pages 197–212 *in* Managed Ecosystems and CO2. Springer Berlin Heidelberg, Berlin/Heidelberg.

Sus, O., M. W. Heuer, T. P. Meyers, and M. Williams. 2013. A data assimilation framework for constraining upscaled cropland carbon flux seasonality and biometry with MODIS. Biogeosciences 10:2451–2466.

Teskey, R. O., and R. E. Will. 1999. Acclimation of loblolly pine (Pinus taeda) seedlings to high temperatures. Tree physiology 19:519–525.

Turner, D. P., G. J. Koerper, and M. E. Harmon. 1995. A carbon budget for forests of the conterminous United States. Ecological Applications 5:421–436.

van Oijen, M., and A. Thomson. 2010. Toward Bayesian uncertainty quantification for forestry models used in the United Kingdom Greenhouse Gas Inventory for land use, land use change, and forestry. Climatic Change 103:55–67.

van Oijen, M., J. Rougier, and R. Smith. 2005. Bayesian calibration of process-based forest models: bridging the gap between models and data. Tree physiology 25:915–927.

Volodin, E. M., N. A. Dianskii, and A. V. Gusev. 2010. Simulating present-day climate with the INMCM4.0 coupled model of the atmospheric and oceanic general circulations. Izvestiya, Atmospheric and Oceanic Physics 46:414–431.

Watanabe, M., T. Suzuki, R. O'ishi, Y. Komuro, S. Watanabe, S. Emori, T. Takemura, M. Chikira, T. Ogura, M. Sekiguchi, K. Takata, D. Yamazaki, T. Yokohata, T. Nozawa, H. Hasumi, H. Tatebe, and M. Kimoto. 2010. Improved Climate Simulation by MIROC5: Mean States, Variability, and Climate Sensitivity. Journal of Climate 23:6312–6335.

Watanabe, S., T. Hajima, K. Sudo, T. Nagashima, T. Takemura, H. Okajima, T. Nozawa, H. Kawase, M. Abe, T. Yokohata, T. Ise, H. Sato, E. Kato, K. Takata, S. Emori, and M. Kawamiya. 2011. MIROC-ESM 2010: model description and basic results of CMIP5-20c3m experiments. Geoscientific Model Development 4:845–872.

Weng, E., and Y. Luo. 2011. Relative information contributions of model vs. data to short‐ and long‐term forecasts of forest carbon dynamics. Ecological Applications 21:1490–1505.

Wertin, T. M., M. A. McGuire, and R. O. Teskey. 2012. Effects of predicted future and current atmospheric temperature and [CO2] and high and low soil moisture on gas exchange and growth of Pinus taeda seedlings at cool and warm sites in the species range. Tree physiology 32:847–858.

Will, R. E., S. M. Wilson, C. B. Zou, and T. C. Hennessey. 2013. Increased vapor pressure deficit due to higher temperature leads to greater transpiration and faster mortality during drought for tree seedlings common to the forest-grassland ecotone. New Phytologist 200:366–374.

Williams, M., P. A. Schwarz, B. E. Law, J. Irvine, and M. R. Kurpius. 2005. An improved analysis of forest carbon dynamics using data assimilation. Global Change Biology 11:89–105.

Wullschleger, S. D., C. A. Gunderson, P. J. Hanson, K. B. Wilson, and R. J. Norby. 2002. Sensitivity of stomatal and canopy conductance to elevated CO2 concentration – interacting variables and perspectives of scale. New Phytologist 153:485–496.

Xu, T., L. White, D. Hui, and Y. Luo. 2006. Probabilistic inversion of a terrestrial ecosystem model: Analysis of uncertainty in parameter estimation and model prediction. Global Biogeochemical Cycles 20:n/a–n/a.

Yukimoto, S., Y. ADACHI, M. HOSAKA, T. SAKAMI, H. YOSHIMURA, M. HIRABARA, T.

Y. TANAKA, E. SHINDO, H. TSUJINO, M. DEUSHI, R. MIZUTA, S. YABU, A. OBATA, H. NAKANO, T. KOSHIRO, T. OSE, and A. KITOH. 2012. A New Global Climate Model of the Meteorological Research Institute: MRI-CGCM3: Model Description and Basic Performance. Journal of the Meteorological Society of Japan 90A:23–64.

Zobitz, J. M., A. R. Desai, D. J. P. Moore, and M. A. Chadwick. 2011. A primer for data assimilation with ecological models using Markov Chain Monte Carlo (MCMC). Oecologia 167:599–611.

Appendix A: Code

```
####Forecasting & Analysis Code for DAPPER results
####Required files to run: Rdata from DAPPER results,
'Tier3_climate_Uofl_METADATA','Tier3_organized.csv'
#### 'Tier3_plotlist_organized_ASW.csv', 'r3pg_interface.so',
'CO2_Conce
ntrations_from_CMIP5_1950-2095'
rm(list = ls())

windows_machine = FALSE
working_directory = '/Users/annikajersild/Documents/Research/3PG/filesformcmc'

#-------------------------------------------------

#--OTHER INFO (WON'T CHANGE UNLESS MODIFY MODEL)-----
npars_used_by_fortran = 59
noutput_variables = 53
npars = 75
sd_index=c(WFiSD = 63,WSiSD = 64,StemNoiSD =
65,WFiSD_exp=66,WSiSD_exp=67,GPP_SD=68,ET_SD=69,Ctran_SD=70) #indexes for the
parameters
fr_index = c(FR1 = 60,FR2 = 61,FR3 = 62) #indexes for the parameters

parnames = c('pFS2','pFS20','StemConst','StemPower','pRx','pRn','SLA0','SLA1','tSLA','k',
        'fullCanAge','MaxIntcptn','LAImaxIntcptn','alpha','MaxCond','LAIgcx','CoeffCond',
        'BLcond','wSx100','thinPower','mF','mR','mS','fracBB0','fracBB1','tBB','gammaFx',
        'gammaF0','tgammaF','Rttover','m0','fN0','TMin','Topt','Tmax','kF','MaxAge',
        'nAge','rAge','y','Density','formFactor','volRatio','Qa','Qb','gDM_mol','molPAR_MJ',
        'FCalpha700',
'fCg700','SWconst1','SWconst2','SWpower1','SWpower2','mort_rate','Alpha_h',
        'pFS_h','pR_h','mort_rate_h','SLA_h','FR Par 1','FR Par 2','FR Par 3','WF SD',
        'WS SD','StemNo SD','WFiSDexp','WSiSDexp','GPP SD','ET SD','Ctrans SD','LAI_SD',
        'FOL_PROD_SD','ROOT_TOTAL_SD','WF_H_SD','WS_H_SD')
#-------------------------------------------------

#---- ENTER THE FORTRAN LIBRARY NAMES HERE ----------
if(windows_machine == TRUE){
  code_library_plot = paste(working_directory,'/source_code/r3pg_interface.dll',sep='')
}else{
  code_library_plot =
'/Users/annikajersild/Dropbox/3PG/code_for_annika_feb5/r3pg_interface.so'
}

setwd(working_directory)
#-------------------------------------------------
```

```
#-----READ IN OBSERVATED DATA-----------------------
observations1 = read.csv(paste(working_directory,'/Tier3_organized.csv',sep=''))

observations1$Treatment = as.factor(observations1$Treatment)
observations1$PlotSizeHa = as.numeric(observations1$PlotSizeHa)
observations1$ind_removed = as.numeric(observations1$ind_removed)
observations1$ind_removed_prop = as.numeric(observations1$ind_removed_prop)


observations = rbind(observations1)
observations = data.frame(PlotID = observations$PlotID,MonthMeas =
observations$MonthMeas,YearMeas = observations$YearMeas,

AgeMeas=observations$AgeMeas,FOL=observations$FOL,WOODY=observations$WOODY,R
OOT_TOTAL=observations$ROOT_TOTAL,

Nha=observations$Nha,ind_removed_prop=observations$ind_removed_prop,WFest_sd=observa
tions$WFest_sd,
                WSest_sd=observations$WSest_sd,GEP = observations$GEP,ET =
observations$ET, Ctrans = observations$Ctrans,
                WOODY_H = observations$WOODY_H,FOL_H =
observations$FOL_H,Ctrans_sd = observations$Ctrans_sd,
                LAI = observations$LAI,FOL_PROD =
observations$FOL_PROD,FOL_PROD_H = observations$FOL_PROD_H,
                FOL_PROD_TOTAL = observations$FOL_PROD_TOTAL, GEP_sd =
observations$GEP_sd, ET_sd = observations$ET_sd,
                WRest_sd = observations$WRest_sd)

observations$ROOT_TOTAL[which(observations$PlotID < 40000)] = -99

#------SITE LEVEL DESCRIPTION DATA--------------------------------

initdata1 = read.csv(paste(working_directory,'/Tier3_plotlist_organized_ASW.csv',sep=''))
initdata1$Treatment = as.factor(initdata1$Treatment)


initdata = rbind(initdata1)
StudyName = initdata$StudyName
Treatment = initdata$Treatment
initdata = data.frame(PlotID = initdata$PlotID,SiteID =
initdata$SiteID,LAT_WGS84=initdata$LAT_WGS84,
                Planting_year = initdata$Planting_year,PlantMonth = initdata$PlantMonth,
                PlantDensityHa = initdata$PlantDensityHa,Initial_ASW = initdata$Initial_ASW,
ASW_min = initdata$ASW_min,
```

```
                ASW_max=initdata$ASW_max,SoilClass = initdata$SoilClass,SI = initdata$SI,FR
= initdata$FR,
                Initial_WF = initdata$Initial_WF,Initial_WS = initdata$Initial_WS,Initial_WR =
initdata$Initial_WR,
                DroughtLevel = initdata$DroughtLevel,DroughtStart = initdata$DroughtStart,
FertFlag=initdata$FertFlag,CO2flag = initdata$CO2flag,
                CO2elev = initdata$CO2elev, ControlPlotID = initdata$ControlPlotID,
                Initial_WF_H = initdata$Initial_WF_H,Initial_WS_H =
initdata$Initial_WS_H,Initial_WR_H = initdata$Initial_WR_H)


initdata$SoilClass=as.character(initdata$SoilClass)
for(i in 1:length(initdata$PlotID)){
  if (initdata$SoilClass[i] == 'S')initdata$SoilClass[i] = 1
  if (initdata$SoilClass[i] == 'SL') initdata$SoilClass[i] = 2
  if (initdata$SoilClass[i] == 'CL')initdata$SoilClass[i] = 3
  if (initdata$SoilClass[i] == 'C')initdata$SoilClass[i] = 4
}
initdata$SoilClass = as.numeric(initdata$SoilClass)
#-----------------------------------------------------------------

#-----ORGANIZE CONTROL PLOT ID (FOR USE WITH EXPERIMENTAL DATA)
plot_index = which(initdata$PlotID == 30049)
#-----------------------------------------------------------------

#-------SELECT WHICH PLOTS TO USE---------------------------------
plotlist = initdata$PlotID[plot_index]   #[which(initdata$PlotID >= 40000)]  #[1:64]
#initdata$PlotID[1:276] #initdata$PlotID[101:112]
StudyName = StudyName[plot_index]
Treatment = Treatment[plot_index]
nplots = length(plotlist)
observations =  observations[observations$PlotID %in% plotlist, ]
initdata = initdata[initdata$PlotID %in% plotlist, ]
#-----------------------------------------------------------------

chain_plot_number = 49

#-----------------------------------------------------------------
#index_guide =
c(pars_start,pars_end,init_Nha_start,init_Nha_end,init_ASW_start,init_ASW_end,FR_start,FR_
end,fol_start,fol_end,
#
stem_start,stem_end,Nha_start,Nha_end,gep_start,gep_end,et_start,et_end,ctrans_start,ctrans_en
d,lai_start,
```

```
#
lai_end,fol_prod_start,fol_prod_end,root_start,root_end,init_WF_start,init_WF_end,init_WS_sta
rt,init_WS_end,
#               init_WR_start,init_WR_end)
#---------------------------------------------------------------

#------PLOT FINAL RESULTS FROM CHAIN-----------------------------
datafilename =
"/Users/annikajersild/Dropbox/3PG/code_for_annika_feb5/control_fert_co2_plots_20mi.1.2016-
02-15.13.38.13.final.Rdata"
load(datafilename,envir=parent.frame())
tmpaccepted = accepted_pars_thinned_burned
pars = array(NA,75)

nmodels = 20
modellist = array(NA,nmodels)
modellist = c('bcc-csm1-1','bcc-csm1-1-m','BNU-ESM', 'CanESM2','CCSM4','CNRM-
CM5','CSIRO-Mk3-6-0','GFDL-ESM2G','GFDL-ESM2M','HadGEM2-CC365','HadGEM2-
ES365','inmcm4','IPSL-CM5A-LR','IPSL-CM5A-MR','IPSL-CM5B-LR','MIROC-
ESM','MIROC-ESM-CHEM','MIROC5','MRI-CGCM3','NorESM1-M')

plotlist = c(30049)#,30041)
statelist = c('VA')#,'OK')
nplots = 1
hucnum = 470 #set to: 1075 for FL, 92      for GA, 470 for VA, 2075 for OK

thin_interval = 100
nyears = 25
nomonths = 12*nyears
PAR = FALSE #True; incorporate parameter uncertainty. False; no parameter uncertainty
(medians)
MOD = TRUE #True; incorporate process model uncertainty. False; no uncertainty
CLIMATE = FALSE #True; incorporate climate model uncertaiont. False; no uncertainty
CO2var = TRUE #True; CO2 varies over time. False; CO2 is held constant
startyearList = c(2006,2070)
nsamples = 100 #Number of iterations for uncertainty

noyears = length(startyearList)

#working_directory = "/Users/annikajersild/Documents/Research/3PG/filesformcmc"
code_library = "/Users/annikajersild/Dropbox/3PG/code_for_annika_feb5/r3pg_interface.so"
npars_used_by_fortran = 59
noutput_variables = 53
npars = 75

StemNoOutput = array(NA,dim=c(nmodels,nplots,noyears,(nyears-2)*12,nsamples))
```

```
WFOutput = array(NA,dim=c(nmodels,nplots,noyears,(nyears-2)*12,nsamples ))
WSOutput = array(NA,dim=c(nmodels,nplots,noyears,(nyears-2)*12,nsamples))
WROutput = array(NA,dim=c(nmodels,nplots,noyears,(nyears-2)*12,nsamples))
TotalOutput = array(NA,dim=c(nmodels,nplots,noyears,(nyears-2)*12,nsamples))

exclude_hardwoods = 1

rcp = 45 #Choose 85 or 45 depending on if you want RCP 8.5 or RCP 4.5

setwd(working_directory)

#Initial Values

#CO2 Data
co2_in = read.csv('CO2_Concentrations_from_CMIP5_1950-2095.csv')

for (model in 1:nmodels){
  #Read in MET Data
  metvar = array(NA,5)
  metvar = c('frost','pr_mm','tasmax_C','tasmin_C','rsds_Wm2')
  met_in_file = array(NA,5)

  modelname = modellist[model]
  print(model)
  print(modelname)
  for (met in 1:5){
    met_in_file[met] =
paste(c('state_rcp',rcp,'_',metvar[met],'_',modelname,'_monthly_2006_2099.csv'),sep="",collapse
="")
  }
  for (plotnum in 1:nplots){
    state = statelist[plotnum]
    metwd =
paste(c('/Users/annikajersild/Documents/Research/3PG/AnnikaProjectMACA/MACA/MACA_
Data_Request_3PG_',state),collapse="")
    setwd(metwd)
    met_in_frost = read.csv(met_in_file[1])
    met_in_pr = read.csv(met_in_file[2])
    met_in_tasmax = read.csv(met_in_file[3])
    met_in_tasmin = read.csv(met_in_file[4])
    met_in_rsds = read.csv(met_in_file[5])


    #observations <- origdata[which(origdata$PlotID == plotlist[plotnum]),]
    init <- initdata[which(initdata$PlotID == plotlist[plotnum]),]
```

```
for (yearnum in 1:length(startyearList)){
  startyear = startyearList[yearnum]
  print(startyear)
  for(parsample in 1:nsamples){
    #Sample from the accepted pars distribution to get our pars
    #HERE BUILD IN THE PARAMETER UNCERTAINTY OPTION if PAR =s
    if (PAR == TRUE){
      sample_index = sample(seq(1,length(tmpaccepted[,1])),1)
      pars = tmpaccepted[sample_index,]
      FR = tmpaccepted[sample_index,(index_guide[7]+chain_plot_number-1)]
    }  else {
        if (MOD==TRUE){
                sample_index = sample(seq(1,length(tmpaccepted[,1])),1)
                for (k in 1:length(tmpaccepted[1,])){
                pars[k] = median(tmpaccepted[,k])}
                par[63] = tmpaccepted[sample_index,63]
                par[64] = tmpaccepted[sample_index,64]
                par[73] = tmpaccepted[sample_index,73]
                FR = median(tmpaccepted[,(index_guide[7]+chain_plot_number-1)])
        }
        else{
      pars = c(NA,length(tmpaccepted[1,]))
      for (k in 1:length(tmpaccepted[1,])){
        pars[k] = median(tmpaccepted[,k])
        FR = median(tmpaccepted[,(index_guide[7]+chain_plot_number-1)])
      }
      }
    }
    fortranpars = pars[1:npars_used_by_fortran]


    PlantedYear = startyear
    InitialYear = startyear+2
    StartAge = 1
    InitialMonth = 1
    EndAge = 25
    StemNum = 1685
    WFi = 1.6
    WRi = .38
    WSi = 1.06
    Initial_WF_H = .01
    Initial_WS_H = .01
    Initial_WR_H = .01
    nomonths = 12*(EndAge-2)

    SI = init$SI
```

```
	Lat = init$LAT_WGS84
	ASWi = init$Initial_ASW
	MaxASW = init$ASW_max
	MinASW = init$ASW_min
	SoilClass = as.character(init$SoilClass)
	if (SoilClass == 'S')SoilClass = 1
	if (SoilClass == 'SL') SoilClass = 2
	if (SoilClass == 'CL')SoilClass = 3
	if (SoilClass == 'C')SoilClass = 4

	MonthMeas =
observations[observations_plot_start[plotnum]:observations_plot_end[plotnum],2]
	YearMeas =
observations[observations_plot_start[plotnum]:observations_plot_end[plotnum],3]

AgeMeas=observations[observations_plot_start[plotnum]:observations_plot_end[plotnum],4]

	site_in = c(PlantedYear, #PlantedYear
		1, #"PlantedMonth"
		InitialYear, #"InitialYear"
		InitialMonth, #"InitialMonth"
		StartAge, #StartAge
		WFi, #"WFi"
		WRi, #"WRi"
		WSi, #"WSi"
		StemNum, #"StemNoi"
		ASWi, #"ASWi"
		Lat, #"Lat"
		FR, #"FR"
		SoilClass, #"SoilClass"
		MaxASW, #"MaxASW"
		MinASW, #"MinASW"
		TotalMonths = nomonths,
		WFi_H = Initial_WF_H,
		WSi_H = Initial_WS_H,
		WRi_H = Initial_WR_H
	)

	site = array(site_in)

	#sitemet <- met_in[which(met_in$Station == plotsites[plotnum]),]
	#years = length(unique(sitemet$Year))

	nometmonths = nyears*12
	met = array(NA,c(nometmonths,6))
	yrnum = startyear - 2006
```

```
endno = (((yrnum*12)+1)+nometmonths)
tmax = met_in_tasmax[hucnum,((yrnum*12)+2):endno]
tmin = met_in_tasmin[hucnum,((yrnum*12)+2):endno]
rain = met_in_pr[hucnum,((yrnum*12)+2):endno]
solar = (met_in_rsds[hucnum,((yrnum*12)+2):endno])/1000000*86400
frost = met_in_frost[hucnum,((yrnum*12)+2):endno]

c02start = startyear
endyear = c02start + nyears-1
if (CO2var == TRUE){
  co2plot = co2_in[which(co2_in >= c02start & co2_in <= endyear),]
  if (rcp == 45){
    co2 = rep(co2plot[,2],each=12 )
  }
  if (rcp == 85){
    co2 = rep(co2plot[,3],each=12 )
  }} else{
    co2plot = co2_in[1,2]
    co2 = rep(co2plot,each=12*25)
  }

met[,1] = t(tmin)  #Tmin
met[,2] = t(tmax)  # Tmax
met[,3] = t(rain) # Rain
met[,4] = t(solar) # SolarRad
met[,5] = t(frost) # FrostDays
met[,6] = t(co2)
met[is.na(met)] <- 0

thin = array(NA,dim=c(1,3))
for(i in 2:2){
  thin[i-1,1]=2006
  thin[i-1,2] = 9
  thin[i-1,3]=0.0
}
nothin = 1

output_dim = noutput_variables  # NUMBER OF OUTPUT VARIABLES
nosite = 15  # LENGTH OF SITE ARRAY
nomet = 6  # NUMBER OF VARIABLES IN METEROLOGY (met)
nopars = length(fortranpars)


#Read in Fortran code
dyn.load(code_library)
```

```
      tmp=.Fortran( "r3pg_interface",
                  output_dim=as.integer(output_dim),
                  met=as.double(t(met)),
                  pars=as.double(fortranpars),
                  site = as.double(site),
                  thin = as.double(thin),
                  out_var=as.double(array(0,dim=c(nomonths,output_dim))),
                  nopars=as.integer(nopars),
                  nomet=as.integer(dim(met)[2]),
                  nosite = as.integer(nosite),
                  nooutputs=as.integer(output_dim),
                  nomonths=as.integer(nomonths),
                  nometmonths = as.integer(dim(met)[1]),
                  nothin = as.integer(dim(thin)[1]),
                  exclude_hardwoods = as.integer(exclude_hardwoods[plotnum]))

      # READ IN FORTRAN OUTPUT FILE PROCESS FORTRAN OUTPUT SO THAT IT
CAN BE COMPARED TO THE DATA

      output =array(tmp$out_var, dim=c(nomonths,output_dim))

      if (MOD == TRUE){
        for(month in 1:nomonths){
          WFOutput[model,plotnum,yearnum,month,parsample] = rnorm(1,mean =
output[month,4], sd = pars[63])
          WSOutput[model,plotnum,yearnum,month,parsample] = rnorm(1,mean =
output[month,6], sd = pars[64]*output[month,6])
          WROutput[model,plotnum,yearnum,month,parsample] =
rnorm(1,mean=output[month,5],sd = pars[73])
        }
      } else {
        #StemNoOutput[model,plotnum,yearnum,,parsample] = output[,7]
        WFOutput[model,plotnum,yearnum,,parsample] = output[,4]
        WSOutput[model,plotnum,yearnum,,parsample] = output[,6]
        WROutput[model,plotnum,yearnum,,parsample] = output[,5]
      }
    }
   }
  }
}


save.image('/Users/annikajersild/Documents/Research/Thesis/ThesisPlots/ModelError_VA.Rdat
a')
paramAge = output[,3]
paramAge2 = paramAge
```

```
paramAge2[276] = 23.7
for (m in 1:nmodels){
  for (y in 1:noyears){
    TotalOutput[m,1,y,,] = WSOutput[m,1,y,,]+WFOutput[m,1,y,,]+WROutput[m,1,y,,]
  }
}

#Part Four: Plot the two different outputs in a chart
if (CLIMATE == FALSE){
  qlinelow = array(NA,dim=c(nmodels,noyears,(nyears-2)*12))
  qlinemedian = array(NA,dim=c(nmodels,noyears,(nyears-2)*12))
  qlinehigh = array(NA,dim=c(nmodels,noyears,(nyears-2)*12))

  qlinelowW = array(NA,dim=c(nmodels,noyears,(nyears-2)*12))
  qlinemedianW = array(NA,dim=c(nmodels,noyears,(nyears-2)*12))
  qlinehighW = array(NA,dim=c(nmodels,noyears,(nyears-2)*12))

  for (m in 1:nmodels){
    for (y in 1:noyears){
      for (i in 1:((nyears-2)*12)){
        qline = quantile(TotalOutput[m,1,y,i,],probs=c(0.025,0.50,0.975))
        qlinelow[m,y,i] = qline[1]
        qlinemedian[m,y,i] = qline[2]
        qlinehigh[m,y,i] = qline[3]
        qlineW = quantile(WSOutput[m,1,y,i,],probs=c(0.025,0.50,0.975))
        qlinelowW[m,y,i] = qlineW[1]
        qlinemedianW[m,y,i] = qlineW[2]
        qlinehighW[m,y,i] = qlineW[3]
      }
    }
  }
} else {
  qlinelow = array(NA,dim=c(noyears,(nyears-2)*12))
  qlinemedian = array(NA,dim=c(noyears,(nyears-2)*12))
  qlinehigh = array(NA,dim=c(noyears,(nyears-2)*12))

  qlinelowW = array(NA,dim=c(noyears,(nyears-2)*12))
  qlinemedianW = array(NA,dim=c(noyears,(nyears-2)*12))
  qlinehighW = array(NA,dim=c(noyears,(nyears-2)*12))


  for (y in 1:noyears){
    for (i in 1:((nyears-2)*12)){
      qline = quantile(TotalOutput[,1,y,i,],probs=c(0.025,0.50,0.975))
      qlinelow[y,i] = qline[1]
      qlinemedian[y,i] = qline[2]
```

```
    qlinehigh[y,i] = qline[3]
    qlineW = quantile(WSOutput[,1,y,i,],probs=c(0.025,0.50,0.975))
    qlinelowW[y,i] = qlineW[1]
    qlinemedianW[y,i] = qlineW[2]
    qlinehighW[y,i] = qlineW[3]
  }
}
```

Appendix B: Supplementary Data

Table B.1: Median Change in biomass at age 25 for each site and type of uncertainty, RCP 8.5. Demonstrates the variation between the median values when each form of uncertainty is incorporated but it is run with each of the different outputs from the climate model data.

Type of Uncertainty Incorporated	VA	FL	OK	GA
Process Model Uncertainty				
bcc-csm1-1	37.822	4.444	7.802	17.596
bcc-csm1-1-m	33.304	19.609	14.07	28.233
BNU-ESM	59.641	16.15	38.028	34.373
CanESM2	31.201	4.923	5.502	12.123
CCSM4	47.681	26.652	33.939	35.546
CNRM-CM5	74.882	28.998	51.727	65.507
CSIRO-Mk3-6-0	57.439	28.507	26.891	40.301
GFDL-ESM2M	47.432	11.903	5.967	33.885
GFDL-ESM2G	58.088	21.703	18.199	31.834
HadGEM2-ES	27.198	-5.943	-1.82	9.659
HadGEM2-CC	32.731	-9.122	7.39	4.985
inmcm4	71.073	42.073	12.3	50.562
IPSL-CM5A-LR	68.093	20.995	20.13	34.696
IPSL-CM5A-MR	41.505	5.043	-0.274	31.263
IPSL-CM5B-LR	56.668	22.489	24.465	33.599
MIROC5	59.811	-15.43	-9.276	24.572
MIROC-ESM	59.935	-30.675	-21.062	11.998
MIROC-ESM-CHEM	71.796	11.109	2.83	45.057
MRI-CGCM3	59.345	42.163	38.394	47.735
NorESM1-M	64.866	21.667	37.965	43.971
Parameter Uncertainty				
bcc-csm1-1	34.855	7.057	-1.651	22.02
bcc-csm1-1-m	32.255	18.301	15.76	20.282
BNU-ESM	58.493	23.811	36.396	41.608
CanESM2	31.894	2.645	-13.189	16.851
CCSM4	44.691	23.238	28.867	29.239
CNRM-CM5	71.759	38.373	47.354	70.302
CSIRO-Mk3-6-0	55.346	35.755	23.57	43.968
GFDL-ESM2M	44.079	11.805	1.642	35.462
GFDL-ESM2G	59.729	15.844	11.299	34.413
HadGEM2-ES	29.877	-8.027	-13.882	5.762
HadGEM2-CC	34.42	-18.085	4.558	-2.753
inmcm4	71.373	35.912	17.192	52.06
IPSL-CM5A-LR	67.6	18.881	11.617	39.991
IPSL-CM5A-MR	43.704	2.23	-2.506	29.201
IPSL-CM5B-LR	57.849	17.421	20.305	35.245
MIROC5	57.313	-26.1	1.007	21.744

MIROC-ESM	61.006	-35.477	-36.258	10.164
MIROC-ESM-CHEM	71.518	15.681	12.332	48.722
MRI-CGCM3	61.984	38.787	39.542	51.676
NorESM1-M	61.546	20.911	51.786	45.955
Climate Model Uncertainty	57.494	18.251	12.665	33.447
All Three – Overall Prediction	51.364	12.225	14.721	31.831

Table B.2*: Standard Deviation in biomass at age 25 for each site and type of uncertainty, RCP 8.5. Demonstrates the variation between the uncertainty values when each form of uncertainty is incorporated but it is run with each of the different outputs from the climate model data.*

Type of Uncertainty Incorporated	**VA**	**FL**	**OK**	**GA**
Process Model Uncertainty				
bcc-csm1-1	13.905	23.446	23.841	33.819
bcc-csm1-1-m	9.787	30.192	21.318	30.324
BNU-ESM	15.014	26.296	24.362	33.501
CanESM2	11.731	26.122	23.9	35.337
CCSM4	13.964	24.845	25.14	28.517
CNRM-CM5	15.51	28.316	22.438	33.158
CSIRO-Mk3-6-0	13.621	21.949	25.504	34.849
GFDL-ESM2M	12.101	25.507	20.371	29.956
GFDL-ESM2G	12.661	27.254	22.806	33.767
HadGEM2-ES	13.812	25.023	19.834	31.966
HadGEM2-CC	10.709	22.912	21.855	34.231
inmcm4	13.799	23.217	22.832	33.673
IPSL-CM5A-LR	14.675	25.153	22.158	35.068
IPSL-CM5A-MR	12.676	24.264	18.847	31.997
IPSL-CM5B-LR	14.283	26.904	23.912	34.507
MIROC5	14.4	21.854	21.025	33.664
MIROC-ESM	16.059	21.203	17.674	34.308
MIROC-ESM-CHEM	17.037	27.785	19.026	35.565
MRI-CGCM3	13.662	29.245	24.159	36.103
NorESM1-M	14.168	24.453	23.557	35.22
Parameter Uncertainty				
bcc-csm1-1	20.878	28.22	49.733	13.359
bcc-csm1-1-m	19.863	28.342	46.259	11.933
BNU-ESM	24.232	27.969	51.81	12.551
CanESM2	20.052	28.127	54.272	12.404
CCSM4	24.125	24.856	55.922	13.36
CNRM-CM5	25.606	31.256	54.546	13.711
CSIRO-Mk3-6-0	17.573	27.439	53.517	12.766
GFDL-ESM2M	23.662	28.473	48.386	13.401
GFDL-ESM2G	21.032	26.692	48.022	13.54
HadGEM2-ES	21.402	29.05	52.271	16.146

HadGEM2-CC	21.217	27.677	48.419	13.547
inmcm4	26.984	26.443	51.485	14.532
IPSL-CM5A-LR	20.654	27.707	49.952	15.434
IPSL-CM5A-MR	22.167	29.26	52.638	14.101
IPSL-CM5B-LR	26.135	30.754	51.115	14.931
MIROC5	24.416	27.22	46.502	12.844
MIROC-ESM	25.47	28.407	57.839	12.919
MIROC-ESM-CHEM	25.35	28.722	55.295	14.355
MRI-CGCM3	23.364	30.03	62.225	12.566
NorESM1-M	25.831	27.329	60.255	13.006
Climate Model Uncertainty	13.941	18.079	17.662	16.614
All Three – Overall Prediction	30.199	41.788	59.475	38.407